

See discussions, stats, and author profiles for this publication at: <https://www.researchgate.net/publication/274258910>

# Mass Spectrometric Characterization of Human Serum Albumin Adducts Formed with N-Oxidized Metabolites of 2-Amino-1-methylphenylimidazo[4,5-b]pyridine in Human Plasma and Hepatocy...

ARTICLE in CHEMICAL RESEARCH IN TOXICOLOGY · MARCH 2015

Impact Factor: 3.53 · DOI: 10.1021/acs.chemrestox.5b00075 · Source: PubMed

---

READS

37

5 AUTHORS, INCLUDING:



**Medjda Bellamri**

Université de Rennes 1

5 PUBLICATIONS 4 CITATIONS

SEE PROFILE



**Sophie Langouët**

French Institute of Health and Medical Research

73 PUBLICATIONS 2,468 CITATIONS

SEE PROFILE



**Robert J Turesky**

University of Minnesota Twin Cities

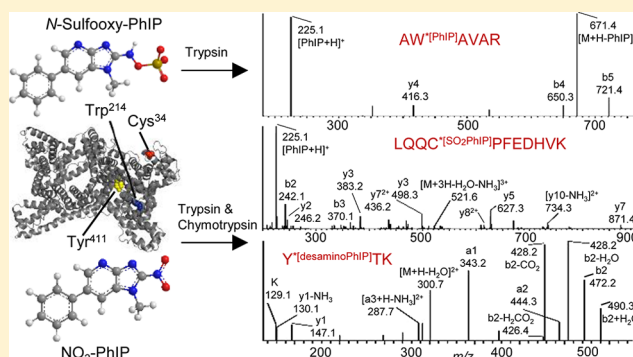
179 PUBLICATIONS 6,115 CITATIONS

SEE PROFILE

Mass Spectrometric Characterization of Human Serum Albumin Adducts Formed with N-Oxidized Metabolites of 2-Amino-1-methylphenylimidazo[4,5-*b*]pyridine in Human Plasma and HepatocytesYi Wang,<sup>†</sup> Lijuan Peng,<sup>‡</sup> Medjda Bellamri,<sup>§,||</sup> Sophie Langouët,<sup>§</sup> and Robert J. Turesky<sup>\*,†</sup><sup>†</sup>Masonic Cancer Center and Department of Medicinal Chemistry, Cancer and Cardiology Research Building, University of Minnesota, 2231 6th Street, Minneapolis, Minnesota 55455, United States<sup>‡</sup>School of Chemical and Environmental Engineering, Wuhan Polytechnic University, ChangQing Garden, Hankou, Wuhan 430023, P. R. China<sup>§</sup>Institut National de la Santé et de la Recherche Médicale (Inserm), U.1085, Institut de Recherche Santé Environnement et Travail (IRSET), Université de Rennes 1, UMS 3480 Biosit, F-35043 Rennes, France<sup>||</sup>ANSES Laboratoire de Fougères, La Haute Marche-Javené, BP 90203, 350302 Fougères, France

## Supporting Information

**ABSTRACT:** 2-Amino-1-methyl-6-phenylimidazo[4,5-*b*]pyridine (PhIP), a carcinogenic heterocyclic aromatic amine formed in cooked meats, is metabolically activated to electrophilic intermediates that form covalent adducts with DNA and protein. We previously identified an adduct of PhIP formed at the Cys<sup>34</sup> residue of human serum albumin following reaction of albumin with the genotoxic metabolite 2-hydroxyamino-1-methyl-6-phenylimidazo[4,5-*b*]pyridine (HONH-PhIP). The major adducted peptide recovered from a tryptic/chymotryptic digest was identified as the missed-cleavage peptide LQQC\*[SO<sub>2</sub>PhIP]PFEDHVK, a [cysteine-S-yl-PhIP]-S-dioxide linked adduct. In this investigation, we have characterized the albumin adduction products of *N*-sulfooxy-2-amino-1-methyl-6-phenylimidazo[4,5-*b*]pyridine (*N*-sulfooxy-PhIP), which is thought to be a major genotoxic metabolite of PhIP formed *in vivo*. Targeted and data-dependent scanning methods showed that *N*-sulfooxy-PhIP adducted to the Cys<sup>34</sup> of albumin in human plasma to form LQQC\*[SO<sub>2</sub>PhIP]PFEDHVK at levels that were 8–10-fold greater than the adduct levels formed with *N*-(acetyloxy)-2-amino-1-methyl-6-phenylimidazo[4,5-*b*]pyridine (*N*-acetoxy-PhIP) or HONH-PhIP. We also discovered that *N*-sulfooxy-PhIP forms an adduct at the sole tryptophan (Trp<sup>214</sup>) residue of albumin in the sequence AW\*[PhIP]AVAR. However, stable adducts of PhIP with albumin were not detected in human hepatocytes. Instead, PhIP and 2-amino-1-methyl-6-(5-hydroxy)phenylimidazo[4,5-*b*]pyridine (5-HO-PhIP), a solvolysis product of the proposed nitrenium ion of PhIP, were recovered during the proteolysis, suggesting a labile sulfenamide linkage had formed between an N-oxidized intermediate of PhIP and Cys<sup>34</sup> of albumin. A stable adduct was formed at the Tyr<sup>411</sup> residue of albumin in hepatocytes and identified as a deaminated product of PhIP, Y\*[desaminoPhIP]TK, where the 4-HO-tyrosine group bound to the C-2 imidazole atom of PhIP.



## INTRODUCTION

2-Amino-1-methyl-6-phenylimidazo[4,5-*b*]pyridine (PhIP) is a carcinogenic heterocyclic aromatic amine (HAA) formed in cooked meat.<sup>1–4</sup> PhIP undergoes metabolic activation by cytochrome P450s, to form 2-hydroxyamino-1-methyl-6-phenylimidazo[4,5-*b*]pyridine (HONH-PhIP).<sup>5,6</sup> HONH-PhIP undergoes esterification by sulfotransferase (SULTs) or *N*-acetyltransferase (NATs) to form the corresponding esters,<sup>7</sup> which undergo heterolytic cleavage to produce the presumed nitrenium ion that binds to DNA.<sup>8,9</sup> The major DNA adduction product of N-oxidized metabolites of PhIP has been

characterized as *N*-(deoxyguanosin-8-yl)-PhIP (dG-C8-PhIP).<sup>10,11</sup> The dG-C8-PhIP adduct has been employed as a biomarker in human studies.<sup>12,13</sup>

The measurement of DNA adducts in human biospecimens remains an analytical challenge because many DNA lesions are repaired and the trace levels of DNA adducts present in tissues may be difficult to measure, even by sensitive LC/MS-based methods.<sup>9,14</sup> The same reactive metabolites of HAAs (or other

Received: February 17, 2015

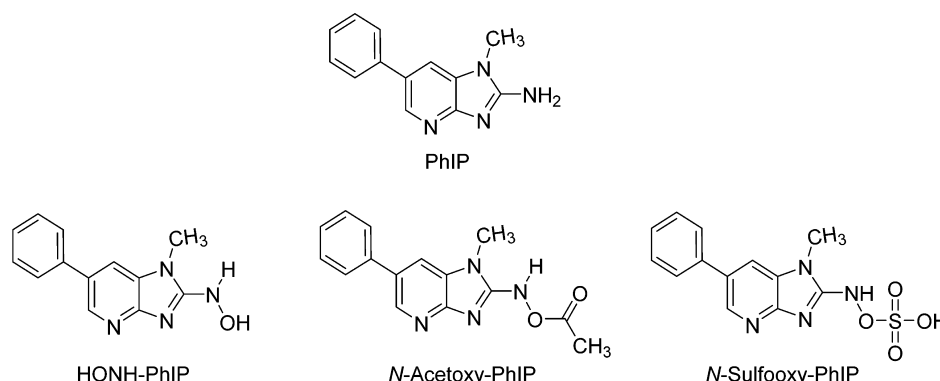


**Figure 1.** Structures of PhIP and N-oxidized metabolites.

procarcinogens) also may bind to proteins to form stable covalent adducts.<sup>15,16</sup> The employment of protein carcinogen adducts as biomarkers is a promising approach to assess exposure to hazardous chemicals because stable covalent protein adducts are not repaired and expected to accumulate during chronic exposure and follow the kinetics of the lifetime of the protein *in vivo*.<sup>17,18</sup>

Hemoglobin (Hb) and serum albumin are the two most abundant proteins in blood and have long life times. The chemistry of reaction of Hb and albumin with many electrophilic genotoxins and toxicants has been investigated.<sup>16,19–21</sup> Like structurally related arylamines, N-oxidation is a major pathway of metabolism of PhIP in humans.<sup>22–24</sup> Hb adducts of aromatic amines are formed by a co-oxidation reaction of the N-hydroxylated arylamine metabolites with oxy-Hb to form the arylnitroso intermediates, which selectively bind at the Hb-Cys<sup>93β</sup> residue and form arylsulfonamide adducts.<sup>18,25,26</sup> Arylsulfonamide adducts are labile and undergo hydrolysis at acidic or alkaline pH to produce the parent arylamine. The labile nature of the Hb arylsulfonamide bond has been exploited to monitor occupational and environmental exposures to a number of primary arylamines.<sup>27</sup> In the case of 4-aminobiphenyl (4-ABP), the structure of the Hb sulfonamide linkage was proven by X-ray crystallography.<sup>28</sup> However, a study with radiolabeled [<sup>14</sup>C]PhIP showed that the level of binding of PhIP to Hb was very low in humans and Hb-PhIP adducts do not appear to be promising candidate biomarkers.<sup>29</sup> In contrast, the binding of PhIP to albumin occurred at levels up to several percent of the ingested dose<sup>29,30</sup> and may be sufficient to biomonitor albumin-PhIP adducts in humans by LC/MS-based methods. However, the structure(s) of the albumin-PhIP adduct(s) formed in humans is unknown.

Human albumin contains only one reduced Cys residue.<sup>31</sup> Cys<sup>34</sup> of albumin is a strong nucleophile and also serves as a powerful antioxidant and scavenger of reactive oxygen species.<sup>21,32</sup> The Cys<sup>34</sup> residues of rodent and human albumin trap reactive electrophiles of HAAs, e.g., 2-amino-3-methylimidazo[4,5-f]quinoline,<sup>33</sup> 2-amino-3,8-dimethylimidazo[4,5-f]quinoxaline,<sup>34</sup> and PhIP,<sup>35–39</sup> and other toxic electrophiles.<sup>21</sup> We have shown that human albumin forms adducts with HONH-PhIP and 2-nitroso-1-methyl-6-phenylimidazo[4,5-b]pyridine (NO-PhIP) at Cys<sup>34</sup> via a sulfonamide linkage.<sup>37,39</sup> N-(Acetoxy)-2-amino-1-methyl-6-phenylimidazo[4,5-b]pyridine (N-acetoxy-PhIP), a metabolite of PhIP that forms covalent DNA adducts,<sup>10,40</sup> reacts with albumin to form an unstable sulfenamide linkage at Cys<sup>34</sup>.<sup>38</sup> We also identified several adducts formed between human albumin and 2-nitro-1-methyl-6-phenylimidazo[4,5-b]pyridine (NO<sub>2</sub>-PhIP).<sup>38</sup>

The formation of covalent adducts of carcinogens with proteins such as albumin is thought to be driven not only by the abundance and relative nucleophilicities of the different amino acid residues available for reaction but also by noncovalent interactions of the reactive metabolite with different receptor regions of proteins, which can direct the sites of carcinogen adduct formation.<sup>41</sup> For example, the major adduct formed between the activated hydroxamic acid of 4-ABP and rat albumin occurred at the sole tryptophan residue, which is situated in a fatty acid binding site in a relatively hydrophobic position deep within the native protein.<sup>42</sup> Studies employing genetically engineered mammalian cell lines expressing human NATs showed that HONH-PhIP is poorly bioactivated by NAT1 and NAT2.<sup>43–45</sup> In comparison, cell lines expressing SULT1A1 were highly effective in the bioactivation of HONH-PhIP, to form the presumed reactive metabolite N-sulfooxy-2-amino-1-methyl-6-phenylimidazo[4,5-b]pyridine (N-sulfooxy-PhIP), which adducted to DNA.<sup>46,47</sup> Thus, the contribution of N-sulfooxy-PhIP to the chemical modification protein (or DNA) may be much greater than that of N-acetoxy-PhIP. N-Sulfooxy-PhIP is appreciably more polar than HONH-PhIP and N-acetoxy-PhIP, and it exists as a negatively charged species at physiological pH. Therefore, the sites of reactivity of N-sulfooxy-PhIP with albumin may be different from other N-oxidized PhIP metabolites.<sup>37–39</sup> To the best of our knowledge, studies of the covalent binding of N-sulfooxy-PhIP with protein or DNA have not been reported.

Our goal is to comprehensively characterize the adduction products of N-oxidized metabolites of PhIP with human albumin and develop albumin-PhIP adducts as biomarkers for molecular epidemiology studies that seek to understand the role of PhIP in human cancer. In this study, we report our findings on the relative reactivity of human albumin with HONH-PhIP, N-acetoxy-PhIP, and N-sulfooxy-PhIP, all of which produce the proposed PhIP nitrenium ion (Figure 1).<sup>8</sup>

## MATERIALS AND METHODS

**Caution.** PhIP is a carcinogen and should be handled in a well-ventilated fume hood with the appropriate protective clothing.

**Chemicals and Materials.** PhIP was purchased from Toronto Research Chemicals (Toronto, ON). 2-Amino-1-methyl-6-[<sup>2</sup>H<sub>5</sub>]-phenylimidazo[4,5-b]pyridine ([<sup>2</sup>H<sub>5</sub>]PhIP, 99% isotopic purity) was a gift from M. Knize and K. Kulp (Lawrence Livermore National Laboratory, Livermore, CA). Human serum albumin, trypsin, chymotrypsin, Pronase E, leucine aminopeptidase, prolidase, *m*-chloroperoxybenzoic acid, and LC/MS grade formic acid were purchased from Sigma-Aldrich (St. Louis, MO). LC/MS grade solvents were purchased from Fisher Scientific (Pittsburgh, PA). All other

chemicals were ACS grade and purchased from Sigma-Aldrich unless stated. Isolute C18 solid-phase extraction (SPE) columns (25 mg) were from Biotage (Charlotte, NC). The Pierce Albumin Depletion Kit was from Thermo Fisher (Rockford, IL). Amicon Ultra centrifugal filter units (10000 molecular weight cutoff) were from Millipore (Billerica, MA). Human plasma was purchased from Bioreclamation LLC (Hicksville, NY).

**Synthesis of HONH-PhIP, N-Acetoxy-PhIP, and 2-Amino-1-methyl-6-(5-hydroxy)phenylimidazo[4,5-b]pyridine (5-HO-PhIP), N-Sulfooxy-PhIP, and N-(Deoxyguanosin-8-yl)-PhIP (dG-C8-PhIP).** The syntheses of HONH-PhIP and N-acetoxy-PhIP were previously reported.<sup>10,38,48</sup> 5-HO-PhIP was obtained by the decomposition of N-acetoxy-PhIP in phosphate buffer (pH 7.4).<sup>35,49</sup> Two methods were employed for the synthesis of N-sulfooxy-PhIP. The first method employed sulfur trioxide/pyridine.<sup>50</sup> HONH-PhIP (5  $\mu$ g, 21 nmol) was reacted with a 1.3-fold molar excess of sulfur trioxide in 50  $\mu$ L of anhydrous pyridine at room temperature for 18 h. The second method was described by Beland and Miller for the synthesis of 2-acetylaminofluorene N-sulfate.<sup>51</sup> A 5-fold molar excess of N,N'-dicyclohexylcarbodiimide (DCCI) dissolved in DMF previously dried over 3 Å molecular sieves was added to HONH-PhIP (5  $\mu$ g, 21 nmol), followed by a H<sub>2</sub>SO<sub>4</sub>/HONH-PhIP molar ratio of 1.2. The mixture was purged with argon and then mixed for 6 h at room temperature. Thereafter, the mixtures were vacuum centrifuged to dryness using a high-vacuum CentriVap Cold Trap (Labconco). The N-sulfooxy-PhIP residues were dissolved in a 1/1 H<sub>2</sub>O/CH<sub>3</sub>CN mixture, sonicated for 1 min, and then immediately subjected to infusion into the MS source, or reacted with DNA or albumin. The UV spectra of HONH-PhIP, N-acetoxy-PhIP, and PhIP were acquired in CH<sub>3</sub>OH, employing an Agilent 8453 spectrophotometer (Agilent Technologies, Santa Clara, CA) (Figure S-1 of the Supporting Information). The spectral data are consistent with previous results.<sup>37</sup> The ESI-MS<sup>n</sup> product ion spectra support the proposed structure of N-sulfooxy-PhIP ([M + H]<sup>+</sup> m/z 321.1  $\rightarrow$  [M + H - SO<sub>3</sub>]<sup>+</sup> m/z 241.1; [M - H]<sup>-</sup> m/z 319.1  $\rightarrow$  [M - H - SO<sub>3</sub>]<sup>-</sup> m/z 239.1). Further mass spectral data are provided (*vide infra*). dG-C8-PhIP and its internal standard, [<sup>13</sup>C<sub>10</sub>]dG-C8-PhIP, were synthesized as described previously.<sup>10,11</sup>

**Trapping N-Sulfooxy-PhIP, N-Acetoxy-PhIP, or HONH-PhIP with 2'-Deoxyguanosine (dG).** The reaction condition of N-acetoxy-PhIP with dG to form dG-C8-PhIP was previously described<sup>10,11</sup> and employed to trap other electrophiles of PhIP in this study. The N-sulfooxy-PhIP (13.4  $\mu$ g, 42 nmol, in 20  $\mu$ L of 50% CH<sub>3</sub>CN), N-acetoxy-PhIP (11.8  $\mu$ g, 42 nmol, in 20  $\mu$ L of CH<sub>3</sub>OH), or HONH-PhIP (10.1  $\mu$ g, 42 nmol, in 20  $\mu$ L of C<sub>2</sub>H<sub>5</sub>OH) was added to a solution of dG [1 mg/mL in 50 mM potassium phosphate buffer (pH 8.0)]. The reaction mixture was agitated at 37 °C for 1 h. Reaction products were applied to an Isolute C18 SPE column, followed by washing the resin with 10% CH<sub>3</sub>OH, and eluting dG-C8-PhIP with 100% CH<sub>3</sub>OH.<sup>11</sup>

**Modification of Human Serum Albumin and Plasma with HONH-PhIP, N-Acetoxy-PhIP, and N-Sulfooxy-PhIP.** Mixed disulfides formed at Cys<sup>34</sup> of albumin were reduced by treatment with  $\beta$ ME.<sup>33</sup> Reduced serum albumin [1 nmol in 300  $\mu$ L of 100 mM potassium phosphate buffer (pH 7.4)] was reacted with HONH-PhIP (3 nmol/10  $\mu$ L of C<sub>2</sub>H<sub>5</sub>OH), N-acetoxy-PhIP (3 nmol/10  $\mu$ L of CH<sub>3</sub>OH), or N-sulfooxy-PhIP (3 nmol/20  $\mu$ L of 50% CH<sub>3</sub>CN). The mixtures were incubated at 37 °C for 12 h (HONH-PhIP) or 3 h (N-acetoxy-PhIP and N-sulfooxy-PhIP) with agitation. The PhIP products unbound to albumin were removed by solvent extraction with a 2 $\times$  volume of ethyl acetate, twice. The albumin solution underwent vacuum centrifugation for 5 min to remove the residual ethyl acetate, and the solution was subjected to a buffer exchange [450  $\mu$ L of 100 mM potassium phosphate buffer (pH 7.4), two times] to remove residual unbound PhIP using centrifugal filters (10000 molecular weight cutoff).

Human plasma (5  $\mu$ L) was diluted with 300  $\mu$ L of 100 mM potassium phosphate buffer (pH 7.4), followed by addition of HONH-PhIP, N-acetoxy-PhIP, or N-sulfooxy-PhIP at a molar ratio of 1/3 (albumin/carcinogen). The mixture was incubated at 37 °C for 12 h, with constant agitation. The albumin was processed as described above. The albumin was purified with the Pierce Albumin Depletion Kit (Pierce Biotechnology, Rockford, IL) employing chromatographic conditions

provided by the supplier. The protein concentration was estimated by measuring the UV absorption at 280 nm (extinction coefficient, 35218 M<sup>-1</sup> cm<sup>-1</sup>).<sup>69</sup>

**PhIP DNA and Albumin Adduct Formation in Human Hepatocytes.** Human liver samples were obtained from patients undergoing liver resection for primary or secondary hepatomas through the Centre de Ressources Biologiques (CRB)-Santé de Rennes (<http://www.crsb-sante-rennes.com>, CHRU Pontchaillou, Rennes, France). The research protocol was conducted under French legal guidelines and the local institutional ethics committee. Hepatocytes were isolated by a two-step collagenase perfusion procedure, and parenchymal cells were seeded in Petri dishes at a density of 3  $\times$  10<sup>6</sup> viable cells/19.5 cm<sup>2</sup> dish in 3 mL of Williams' modified medium, except that bovine serum albumin was replaced with human albumin pre-reduced with  $\beta$ ME (1 g/L).<sup>52</sup> The cells were then incubated with PhIP (50  $\mu$ M) or a PhIP/[<sup>2</sup>H<sub>5</sub>]PhIP mixture (1/1, 50  $\mu$ M) for 24 h. The cells were retrieved from the Petri dishes and pelleted by centrifugation.

**PhIP DNA Adduct Measurements in Human Hepatocytes by UPLC-ESI/MS<sup>3</sup>.** DNA was isolated by chloroform/phenol extraction, and dG-C8-PhIP was quantitated by UPLC-ESI/MS<sup>3</sup>.<sup>11,52</sup> [<sup>13</sup>C<sub>10</sub>]dG-C8-PhIP was employed as an internal standard and spiked into DNA prior to enzymatic digestion at a level of one adduct per 10<sup>6</sup> DNA bases. The analyses were conducted with a Waters NanoAcquity UPLC system (Waters Corp., New Milford, MA) equipped with a Waters Symmetry trap column (180  $\mu$ m  $\times$  20 mm, 5  $\mu$ m particle size), a Michrom C18 AQ column (0.3 mm  $\times$  150 mm, 3  $\mu$ m particle size), and a Michrom CaptiveSpray source interfaced with a linear quadrupole ion trap mass spectrometer (LTQ Velos, Thermo Fisher, San Jose, CA), employing chromatographic conditions and MS data acquisition parameters as described previously.<sup>52</sup>

**Albumin Isolation and Proteolytic Digestion.** The albumin in the cell culture media of hepatocytes was extracted twice with 2 volumes of ethyl acetate to remove unmetabolized PhIP, and then the aqueous phase was precipitated with 2 volumes of chilled ethanol. The precipitated albumin was centrifuged and resuspended in 0.3 mL of 100 mM potassium phosphate buffer (pH 7.4). The protein was then isolated by the Albumin Depletion Kit as described above, followed by desalting using Millipore centrifugal filters (10000 molecular weight cutoff).

**Trypsin/Chymotrypsin Digestion.** Albumin [50  $\mu$ g in 200  $\mu$ L of 50 mM ammonium bicarbonate buffer (pH 8.5)] was digested with trypsin (1/50, w/w, protease/protein) and chymotrypsin (1/25, w/w, protease/protein), which were dissolved in 1 mM HCl containing 2 mM CaCl<sub>2</sub>. The mixture was incubated at 37 °C for 20 h. For the denaturation of albumin, the protein (50  $\mu$ g) was resuspended in 0.25 M Tris buffer (pH 7.4) containing 8 M urea. Dithiothreitol (DTT) (1.5 mg, 20 mM) was added to the solution, and the mixture was incubated at 55 °C for 1 h, followed by addition of iodoacetamide (IAA) (6 mg, 65 mM). The mixture was incubated in the dark at 22 °C for 1 h. Excess DTT and IAA were removed using centrifugal filters. The albumin was dissolved in 200  $\mu$ L of 50 mM ammonium bicarbonate buffer (pH 8.5) and subjected to proteolytic digestion as described above. After digestion, the mixture was diluted with 10 volumes of distilled water and applied to an Isolute C18 SPE column. Polar peptides were removed with 10% CH<sub>3</sub>OH (2 mL), and adducts were eluted with CH<sub>3</sub>OH (1 mL), followed by concentration to dryness by vacuum centrifugation.

**Trypsin Digestion.** Denatured or nondenatured PhIP-modified albumin [50  $\mu$ g in 200  $\mu$ L of 50 mM ammonium bicarbonate buffer (pH 8.5)] was digested with trypsin (1/50, w/w, protease/protein). The mixture was incubated at 37 °C for 20 h, followed by SPE purification as described above.

**Pronase E/Leucine Aminopeptidase/Prolidase Digestion.** Unmodified or PhIP-modified albumin [50  $\mu$ g in 200  $\mu$ L of 50 mM ammonium bicarbonate buffer (pH 8.5)] was digested with Pronase E (1/2, w/w, protease/protein), leucine aminopeptidase (1/30, w/w, protease/protein), and prolidase (1/8, w/w, protease/protein). The mixture was incubated at 37 °C for 20 h, followed by SPE purification as described above.



**Mass Spectral Measurements of PhIP Metabolites and Ultraperformance Liquid Chromatography–Electrospray Ionization Multistage Mass Spectrometry (UPLC–ESI/MS<sup>n</sup>) for Albumin-PhIP Adducts.** Mass spectral data of metabolites and synthetic peptides LQQCPF (New England Inc., Gardner, MA) were acquired by infusion with an Orbitrap Elite<sup>TM</sup> Hybrid Ion Trap Orbitrap mass spectrometer (Thermo Fisher) and a Michrom Bioresource Inc. (Auburn, CA) Advance CaptiveSpray source. Typical instrument tuning parameters were as follows: capillary temperature, 270 °C; source spray voltage, 2 kV for positive ion mode and 1.5 kV for negative ion mode; S-lens RF level, 69%; skimmer offset voltage, 0 V; source fragmentation, 5 V. Helium, set at 1 mTorr, was used as the collision and damping gas in the ion trap. There was no sheath or auxiliary gas. All analyses were conducted in the positive ionization mode except for the characterization of the *N*-sulfooxy-PhIP. The isolation width was set at  $m/z$  1 for the MS<sup>2</sup> and MS<sup>3</sup> scan modes; the activation  $Q$  was set at 0.35, and the activation time was 10 ms.

The UPLC–ESI/MS<sup>n</sup> system consists of a Dionex Ultimate 3000 LC instrument (Thermo Scientific, Waltham, MA) and an Orbitrap Elite<sup>TM</sup> Hybrid Ion Trap Orbitrap mass spectrometer. The peptides of the albumin digest were resolved with a Magic C18AQ column (0.3 mm × 150 mm, Michrom Bioresource Inc.) with a 25 min (targeted MS/MS) or 60 min (data-dependent scanning) gradient starting from 100% solvent A (5% CH<sub>3</sub>CN with 0.01% HCO<sub>2</sub>H) to 100% solvent B (95% CH<sub>3</sub>CN with 0.01% HCO<sub>2</sub>H) at a flow rate of 5  $\mu$ L/min. The Chromeleon 7.2 Chromatography Data System was used for the HPLC management. The Advance CaptiveSpray was employed as the ion source, and parameters were set as follows: capillary temperature, 270 °C; ionization voltage, 2 kV for positive ion mode; in-source fragmentation, 5 V; one microscan; maximal injection time, 10 ms for MS and 50 ms for MS<sup>n</sup>; MS fragmentation, a normalized collision energy of 35%; no auxiliary and sheath gases used. The isolation width was set at  $m/z$  1 for both MS<sup>2</sup> and MS<sup>3</sup> scan modes, and the activation  $Q$  was set at 0.35. AGC (automated gain control) was set 30000 for ion trap (IT) MS and 10000 for IT MS<sup>n</sup>, 10<sup>6</sup> for Orbitrap (FT) MS, and 50000 for FT. The Orbitrap was routinely calibrated in positive and negative ion modes using Pierce LTQ Velos ESI Positive Ion Calibration Solution (2  $\mu$ g/mL caffeine, 1  $\mu$ g/mL MRFA, 0.001% Ultramark 1621, and 0.00005% *n*-butylamine) and Pierce ESI Negative Ion Calibration Solution (2.9  $\mu$ g/mL sodium dodecyl sulfate, 5.4  $\mu$ g/mL sodium taurocholate, and 0.001% Ultramark 1621) (Pierce Biotechnology).

For the mass tag-triggered data-dependent acquisition method, a full MS scan (mass range, 100–1800 Da) was obtained, followed by five data dependent scans (mass range, 100–1800 Da), which were triggered by a pattern of the unlabeled PhIP to [<sup>2</sup>H<sub>5</sub>]PhIP adducts at a partner intensity ratio of 65–100%, by enabling the mass tags option ( $m/z$  5, 2.5, or 1.67 for singly, doubly, or triply charged ions, respectively).<sup>38</sup> The MS/MS spectra were recorded using dynamic exclusion of previously analyzed precursors for 180 s with a repeat of 3 and a repeat duration of 60 s. CID was selected for ion fragmentation with a normalized collision energy of 35%. The maximal injection time of MS/MS was set at 50 ms, and the isolation width was set as  $m/z$  2.

**Data Analysis.** Xcalibur version 2.2 was employed for data acquisition and data processing. Peptide adducts were identified manually and facilitated by MyriMatch (version 2.1.140)<sup>53,54</sup> using a 31-protein subset database containing albumin from an initial search against the RefSeq human protein database, version 37.3. MyriMatch was configured to have Cys to contain carbamidomethyl (+57.0 Da) for IAA treatment or (+32.0 or +48.0 Da) for oxidation of Cys to the sulfinic or sulfonic acids, and to allow for the possibility of oxidation (+16.0 Da) on methionines and deamidation (−17.0 Da) of N-terminal glutamines. Peptides modified with HONH-PhIP and HONH-[<sup>2</sup>H<sub>5</sub>]PhIP were allowed to have dynamic modifications at [C,K,Y,S,T,W,H] of 222.1 (HONH-PhIP – H<sub>2</sub>O) and 227.1 Da (HONH-[<sup>2</sup>H<sub>5</sub>]PhIP – H<sub>2</sub>O), or dynamic modifications at [C] of 238.1 and 243.1 Da for adduction with nitroso-PhIP (sulfonamide adducts) and 254.1 and 259.1 Da (sulfonamide adducts). Candidate peptides were allowed to have trypsin cleavages or protein termini at one or both termini (semitryptic search), and up to two missed cleavages were permitted. The precursor error was set at  $m/z$  1.25, but fragment ions were required to match within  $m/z$  0.5. Analyses of modified albumin were also performed with trypsin/chymotrypsin

digests, employing the same configurations. The IDPicker algorithm version 3.0.634 filtered the identifications for each spectrum with a 2% identification false discovery rate at the peptide spectrum match level.

## RESULTS

**Characterization of HONH-PhIP, *N*-Acetoxy-PhIP, and *N*-Sulfooxy-PhIP.** The UV spectra of PhIP, HONH-PhIP, and *N*-acetoxy-PhIP are provided in Figure S-1 of the Supporting Information. Because of its instability, the *N*-sulfooxy-PhIP could not be isolated and characterized by UV or online UPLC–MS analysis. Therefore, the yield of synthesis could not be determined. *N*-Sulfooxy-PhIP underwent rapid hydrolysis once it was dissolved in an aqueous solution, and only HONH-PhIP was detected by HPLC. The sulfate ester of *N*-hydroxy-*N*-acetyl-2-aminofluorene was also reported to be highly unstable in an aqueous solution.<sup>51</sup> In contrast, *N*-acetoxy-PhIP had sufficient stability to be assayed by UPLC–MS and UV measurement.<sup>38</sup> The full scan mass spectra of HONH-PhIP, *N*-acetoxy-PhIP, and *N*-sulfooxy-PhIP, acquired by infusion, are shown in panels A–C of Figure 2, respectively. The protonated ions [ $M + H$ ]<sup>+</sup> are observed for HONH-PhIP (observed at  $m/z$  241.1081 vs calculated at  $m/z$  241.1084) and *N*-acetoxy-PhIP (observed at  $m/z$  283.1192 vs calculated at  $m/z$  283.1190); however, the *N*-sulfooxy-PhIP underwent extensive hydrolysis, and the protonated ion was present at extremely low abundance ([ $M + H$ ]<sup>+</sup> at  $m/z$  321.0647 vs calculated at  $m/z$  321.0652). The base peak of *N*-sulfooxy-PhIP was observed at  $m/z$  223.0979 (calculated at  $m/z$  223.0978) in the full scan mass spectrum (Figure 2A) and assigned as the nitrenium ion ([ $M + H - H_2SO_4$ ]<sup>+</sup>). The relative abundance of the ion at  $m/z$  223.0979 in Figure 2A was considerably greater than that observed in the full scan mass spectra of *N*-acetoxy-PhIP and HONH-PhIP (Figure 2B,C), an observation consistent with the labile nature of the *N*-sulfooxy linkage of *N*-sulfooxy-PhIP. The minor ion present in the full scan spectrum of *N*-sulfooxy-PhIP at  $m/z$  208.0866 (calculated at  $m/z$  208.0869) is consistent with in-source fragmentation and loss of hydroxylamine-*O*-sulfonic acid [ $NH_2OSO_3H$ ]. Further fragmentation of the nitrenium ion ( $m/z$  223.0979) produces the ions at  $m/z$  196.0866 (calculated at  $m/z$  196.0869) [loss of HCN] and  $m/z$  179.0601 (calculated at  $m/z$  179.0604) [loss of HCN + NH<sub>3</sub>] (Figure 2A).

The product ion spectra of *N*-acetoxy-PhIP and HONH-PhIP are consistent with the spectral data in the literature.<sup>38</sup> *N*-Acetoxy-PhIP (observed at  $m/z$  283.1192) undergoes CID with losses of C<sub>2</sub>H<sub>3</sub>O<sub>2</sub> (observed at  $m/z$  224.1057 vs calculated at  $m/z$  224.1057) to form the PhIP radical cation, and C<sub>2</sub>H<sub>4</sub>O<sub>2</sub> (observed at  $m/z$  223.0981 vs calculated at  $m/z$  223.0978) to form PhIP nitrenium ion (Figure S-2A of the Supporting Information). CID studies with HONH-PhIP and 1-[<sup>2</sup>H<sub>3</sub>C]-HONH-PhIP have shown that nitrenium ion formation in the gas phase occurs primarily by homolytic cleavages at the hydrogen atom bonded to the C1 methyl atom and the HO-N<sup>2</sup> bond of HONH-PhIP.<sup>55</sup> This species may rearrange to form a pyrazine ring,<sup>56</sup> which undergoes fragmentation to produce ions at  $m/z$  206.0713, 196.0870, and 179.0605 as described in the Supporting Information. These fragment ions are observed in the product ion spectra of *N*-acetoxy-PhIP (Figure S-2B of the Supporting Information) and HONH-PhIP (data not shown).

The deprotonated ion of *N*-sulfooxy-PhIP [ $M - H$ ]<sup>−</sup> was observed in negative ion mode at  $m/z$  319.0499 (calculated at  $m/z$  319.0506) (Figure 2D) and undergoes fragmentation to form the HONH-PhIP [ $M - H - SO_3$ ]<sup>−</sup> ion at  $m/z$  239.0939

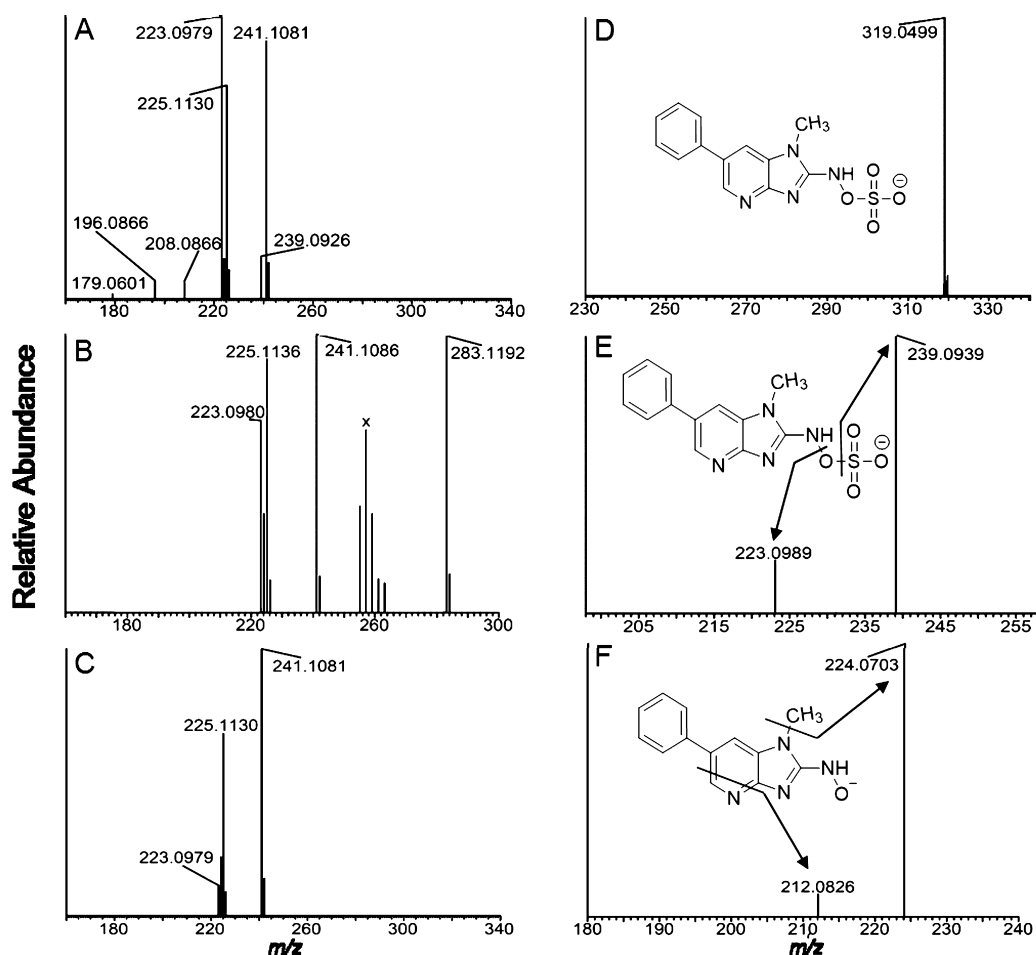


**Figure 2.** ESI-MS full scan mass spectra of (A) *N*-sulfooxy-PhIP ( $m/z$  321.0652), (B) *N*-acetoxy-PhIP ( $m/z$  283.1190), and (C) HONH-PhIP ( $m/z$  241.1084) in positive ion mode. The ion observed at  $m/z$  225.1130 is attributed to PhIP and occurs by in-source reduction of HONH-PhIP. (D) Product ion spectrum of *N*-sulfooxy-PhIP ( $[M - H]^-$   $m/z$  319.0506 acquired at 0 collision energy, isolation width of  $m/z$  1). (E) Product ion spectra of *N*-sulfooxy-PhIP ion at  $m/z$  319.1. (F) Product ion spectra of *N*-sulfooxy-PhIP at the  $MS^3$  scan stage ( $m/z$  319.0 >  $m/z$  239.1 >) in negative ion mode. The cluster of ions designated X between  $m/z$  255 and 263 in the full scan mass spectrum of *N*-acetoxy-PhIP (B) consists of background ions present in the reaction medium.

(calculated at  $m/z$  239.0938) (Figure 2E). The product ion spectrum of the *N*-sulfooxy-PhIP at the  $MS^3$  scan stage ( $m/z$  319.1 >  $m/z$  239.1 >) displays a radical anion at  $m/z$  224.0703 (calculated at  $m/z$  224.0704), attributed to a loss of  $CH_3^\bullet$  from HONH-PhIP (Figure 2F). These mass spectral data support the proposed structure being *N*-sulfooxy-PhIP.

**Trapping Reactive N-Oxidized Electrophiles of PhIP with dG.** dG was used to trap the electrophilic N-oxidized metabolites of PhIP, by formation of dG-C8-PhIP, which was monitored by UPLC-ESI/MS<sup>n</sup>.<sup>11,52</sup> The relative amounts of dG-C8 adduct formation were based on the total ion counts of dG-C8-PhIP adduct acquired at the  $MS^3$  scan stage. Representative chromatograms and the product ion spectrum are shown in Figure S-3 of the Supporting Information. The spectrum is in excellent agreement with our previously published data.<sup>11</sup> The greatest amount of dG-C8-PhIP formation occurred with *N*-acetoxy-PhIP, followed by *N*-sulfooxy-PhIP, and then HONH-PhIP (Figure 3). There was no significant difference between the peak area ion counts of dG-C8-PhIP obtained by the reaction of dG with the two different synthetic preparations of *N*-sulfooxy-PhIP ( $p = 0.633$ ;  $t$  test). The dG-C8-PhIP adduct level obtained with *N*-sulfooxy-PhIP was 10–13 times greater than the adduct level formed with HONH-PhIP ( $p < 0.005$ ;  $t$  test), providing further evidence of the existence of the reactive

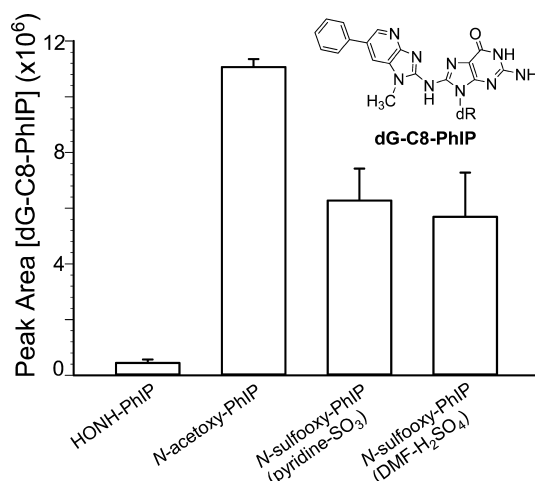


**Figure 3.** Peak area counts of dG-C8-PhIP adducts at the  $MS^3$  scan stage ( $m/z$  490.1 >  $m/z$  374.3 >) from the reaction of dG with HONH-PhIP, *N*-acetoxy-PhIP, *N*-sulfooxy-PhIP (pyridine- $SO_3$ ), or *N*-sulfooxy-PhIP ( $DMF-H_2SO_4$ ). Data are from three independent measurements (mean  $\pm$  SD;  $n = 3$ ).

*N*-sulfooxy-PhIP electrophile. The lower level of dG-C8-PhIP obtained by reaction of dG with *N*-sulfooxy-PhIP than

*N*-acetoxy-PhIP could be explained by the unstable nature of *N*-sulfooxy-PhIP, which undergoes extensive solvolysis during the reaction with dG. We could not measure *N*-sulfooxy-PhIP and assumed that the yield of the synthesis was quantitative. However, the yield of *N*-sulfooxy-PhIP may have been considerably lower and resulted in smaller amounts of dG-C8-PhIP formed, although, as reported below, the level of albumin Cys<sup>34</sup> adduct formation was greater with *N*-sulfooxy-PhIP than with *N*-acetoxy-PhIP.

**Data-Dependent and Targeted Mass Spectrometric Characterization of Albumin Cys<sup>34</sup> Adducts with *N*-Oxidized Metabolites of PhIP: [2H<sub>5</sub>]PhIP.** Adducts of PhIP formed with commercial albumin and albumin in human plasma modified with a 3-fold molar excess of the *N*-sulfooxy-PhIP/*N*-sulfooxy-[2H<sub>5</sub>]PhIP, *N*-acetoxy-PhIP/*N*-acetoxy-[2H<sub>5</sub>]PhIP, or HONH-PhIP/HONH-[2H<sub>5</sub>]PhIP mixture (each at a 1:1 molar ratio), following digestion with trypsin and chymotrypsin, were characterized by data-dependent scanning.<sup>38,39</sup> The Xcalibur software was programmed to switch from the full survey scan MS to the MS/MS scan mode, which was triggered by the characteristic isotopic pattern of unlabeled PhIP: [2H<sub>5</sub>]PhIP at a partner intensity ratio of 65–100%.<sup>38</sup> This wide tolerance for the partner intensity was employed because the deuterium isotope effect caused the [2H<sub>5</sub>]PhIP-peptide adducts to elute ~2 s earlier than the unlabeled adducts in some instances, resulting in a distortion of the 1:1 ratio of unlabeled PhIP to [2H<sub>5</sub>]PhIP adducts.<sup>38</sup> The MyriMatch search program and manual verification of the isotope tags resulted in the identification of three Cys<sup>34</sup> peptide adducts previously characterized with HONH-PhIP and *N*-acetoxy-PhIP: the single missed cleavage sulfinamide LQQC\*[SOPHIP]PFEDHVK ([M + 3H]<sup>3+</sup> at *m/z* 527.1), the single missed cleavage sulfonamide LQQC\*[SO<sub>2</sub>PhIP]PFEDHVK ([M + 3H]<sup>3+</sup> at *m/z* 533.2), and the fully digested sulfinamide LQQC\*[SOPHIP]PF ([M + 2H]<sup>2+</sup> at *m/z* 487.2) (Table 1).<sup>38</sup> LQQC\*[SOPHIP]PFEDHVK

**Table 1. Identified Peptide Adducts from *N*-Sulfooxy-PhIP and *N*-Sulfooxy-[2H<sub>5</sub>]PhIP, *N*-Acetoxy-PhIP, and *N*-Acetoxy-[2H<sub>5</sub>]PhIP, or HONH-PhIP and HONH-[2H<sub>5</sub>]PhIP Modified Albumin Using the Mass Tag-Triggered Data-Dependent Scanning Method<sup>a</sup>**

proteolytic enzymes	peptide adducts	modified sites
trypsin/chymotrypsin	LQQC*[SOPHIP]PFEDHVK	Cys <sup>34</sup>
	LQQC*[SO <sub>2</sub> PhIP]PFEDHVK	Cys <sup>34</sup>
	LQQC*[SOPHIP]PF	Cys <sup>34</sup>
	C*[SO <sub>2</sub> PhIP]	Cys <sup>34</sup>
Pronase E/leucine aminopeptidase/prolidase	C*[SO <sub>2</sub> PhIP]PF	Cys <sup>34</sup>
	W <sup>[PhIP]</sup>	Trp <sup>214</sup>
	H <sup>[PhIP]</sup>	His

<sup>a</sup>The His residues of SA that reacted with *N*-oxidized PhIP are uncertain. There are 16 His residues in SA, and the His-containing PhIP adduct(s) was identified as a mono amino acid adduct following Pronase digestion.

elutes at ~28 min, followed by LQQC\*[SO<sub>2</sub>PhIP]PFEDHVK (*t<sub>R</sub>* = 31 min) and LQQC\*[SO<sub>2</sub>PhIP]PF (*t<sub>R</sub>* = 34 min). The mass tag data-dependent acquisition method searched by MyriMatch or manual searching did not identify other adducts in the tryptic/chymotryptic digests of albumin modified with *N*-sulfooxy-PhIP or other *N*-oxidized PhIP metabolites. Thus, similar to the results previously

obtained by reaction of HONH-PhIP or *N*-acetoxy-PhIP with human albumin,<sup>38</sup> Cys<sup>34</sup> is the major nucleophilic amino acid residue of albumin that reacts with *N*-sulfooxy-PhIP.

A representative mass chromatogram of albumin-Cys<sup>34</sup> peptide adducts formed with *N*-sulfooxy-PhIP is shown in Figure 4 along with the higher-energy collision dissociation (HCD) product ion spectra (LQQC\*[SOPHIP]PF, [M + 2H]<sup>2+</sup> at *m/z* 487.2; LQQC\*[SOPHIP]PFEDHVK, [M + 3H]<sup>3+</sup> at *m/z* 527.9; and LQQC\*[SO<sub>2</sub>PhIP]PFEDHVK, [M + 3H]<sup>3+</sup> at *m/z* 533.2). The product ion spectrum of the sulfinamide LQQC\*[SOPHIP]PF contains two major ions, PhIP (*m/z* 225.1) and [M + H – PhIP]<sup>+</sup> (*m/z* 749.1) (Figure 4A). The protonated ion of PhIP is also the base peak in the product ion spectrum of LQQC\*[SOPHIP]PFEDHVK (Figure 4B). The sulfonamide-linked adduct is considerably more stable toward HCD and CID, and a majority of *–b* and *–y* ions are seen in both HCD and CID product ion spectra; protonated PhIP (*m/z* 225.1) is the base peak in the HCD product ion spectrum of LQQC\*[SO<sub>2</sub>PhIP]PFEDHVK (Figure 4C), but a minor ion in the CID product ion spectrum.<sup>38</sup>

The relative amounts of LQQC\*[SOPHIP]PF and LQQC\*[SO<sub>2</sub>PhIP]PFEDHVK adducts formed by reaction of human albumin or human plasma with *N*-sulfooxy-PhIP, *N*-acetoxy-PhIP, or HONH-PhIP were determined by targeted UPLC–ESI/MS<sup>2</sup>. There was no statistically significant difference between the level of the LQQC\*[SOPHIP]PF formed by *N*-sulfooxy-PhIP, *N*-acetoxy-PhIP, or HONH-PhIP in either albumin in human plasma samples or commercial human albumin (*p* = 0.231; one-way ANOVA) (unpublished results, Y. Wang). However, the amount of LQQC\*[SO<sub>2</sub>PhIP]PFEDHVK recovered from *N*-sulfooxy-PhIP-modified human plasma was 2 times greater than the amounts formed with *N*-acetoxy-PhIP- and HONH-PhIP-modified samples (*p* < 0.05; *t* test). There was no significant difference between LQQC\*[SO<sub>2</sub>PhIP]PFEDHVK levels produced by *N*-acetoxy-PhIP and HONH-PhIP (*p* > 0.05; *t* test) (unpublished results, Y. Wang).

**Identification of the Albumin Trp<sup>214</sup> Adduct of PhIP at AW\*[PhIP]AVAR.** The sole tryptophan residue of rat albumin, Trp<sup>214</sup>, was reported to bind to the genotoxic metabolite *N*-sulfonyloxy-*N*-acetyl-4-aminobiphenyl.<sup>42</sup> Human albumin also contains one sole Trp, which resides at the same sequence location as for rat albumin.<sup>31</sup> We sought to determine whether the Trp<sup>214</sup> of human albumin had reacted with the *N*-sulfooxy-PhIP to form an adduct that had escaped detection by the mass tag-triggered data-dependent acquisition method. Human albumin and human plasma modified with *N*-sulfooxy-PhIP were monitored for AW\*[PhIP]AVAR ([M + 2H]<sup>2+</sup> at *m/z* 448.2), by targeted UPLC–ESI/MS<sup>2</sup>, following digestion of albumin with trypsin. The mass chromatogram and product ion spectrum of the adduct from plasma albumin, obtained by accurate mass measurements with the Orbitrap, are shown in panels A and B of Figure 5. The product ion spectrum of AW\*[PhIP]AVAR ([M + 2H]<sup>2+</sup> at *m/z* 448.2) contains predominant ions assigned to protonated PhIP (*m/z* 225.1) and [M + H – PhIP]<sup>+</sup> (*m/z* 671.4), with minor ions assigned as *–b* ions [*m/z* 650.3 (*b*<sub>4</sub>), *m/z* 721.4 (*b*<sub>5</sub>)] and *–y* ion at *m/z* 416.3 (*y*<sub>4</sub>). The ion attributed to protonated PhIP and the *–b* and *–y* ions were within 2.3 ppm of the calculated values.

The plasma PhIP albumin peptide adducts recovered from optimized enzyme digestion conditions are depicted in Figure 5C. In the absence of stable, isotopically labeled internal standards,

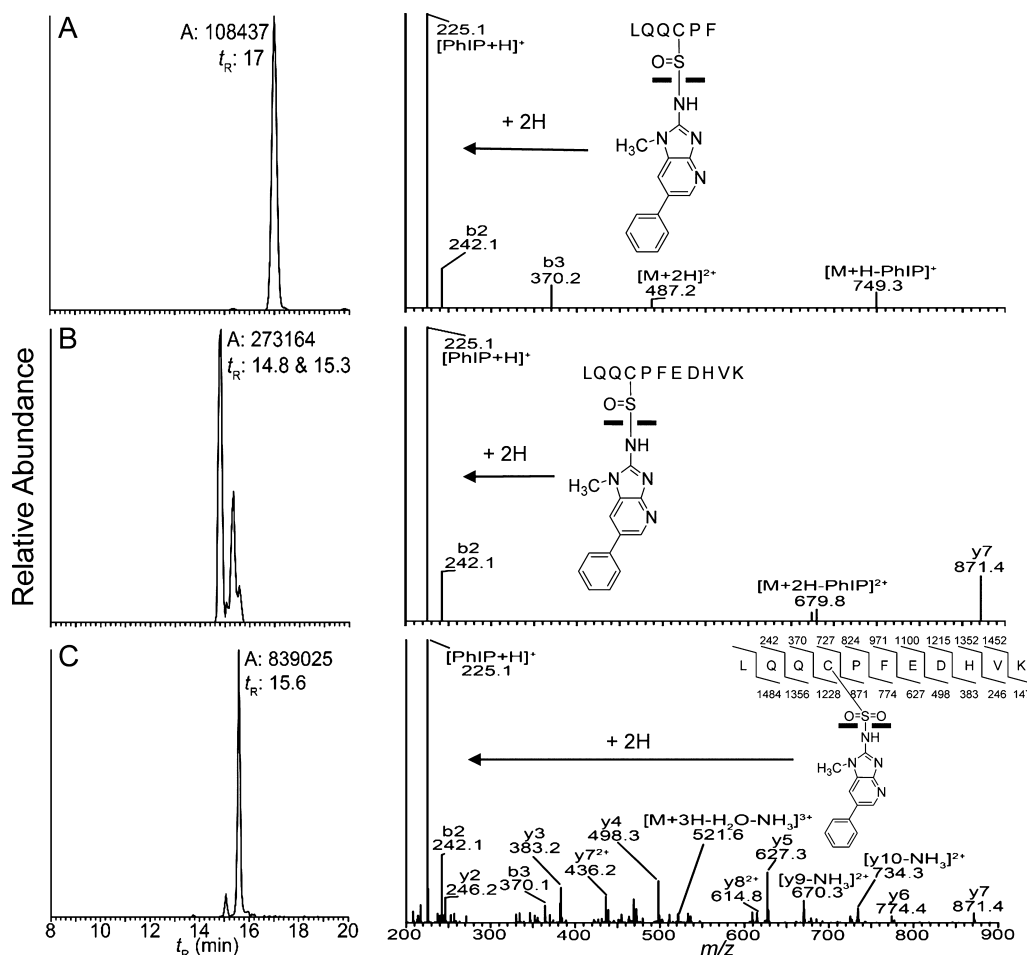


**Figure 4.** Reconstructed mass chromatograms (left) and product ion spectra (right) of Cys<sup>34</sup> adducts from N-sulfooxy-PhIP-treated human plasma (left) of (A) LQQC\*[SOPhIP]PF ( $[M+2H]^{2+}$  at  $m/z$  487.2 >  $m/z$  225.1), (B) LQQC\*[SOPhIP]PFEDHVK ( $[M+3H]^{3+}$  at  $m/z$  527.9 >  $m/z$  225.1), and (C) LQQC\*[SO<sub>2</sub>PhIP]PFEDHVK ( $[M+3H]^{3+}$  at  $m/z$  533.2 >  $m/z$  225.1) and corresponding HCD product ion spectra (right), following tryptic/chymotryptic digestion of albumin.  $t_R$  is the retention time; A is the area ion counts of the peak.

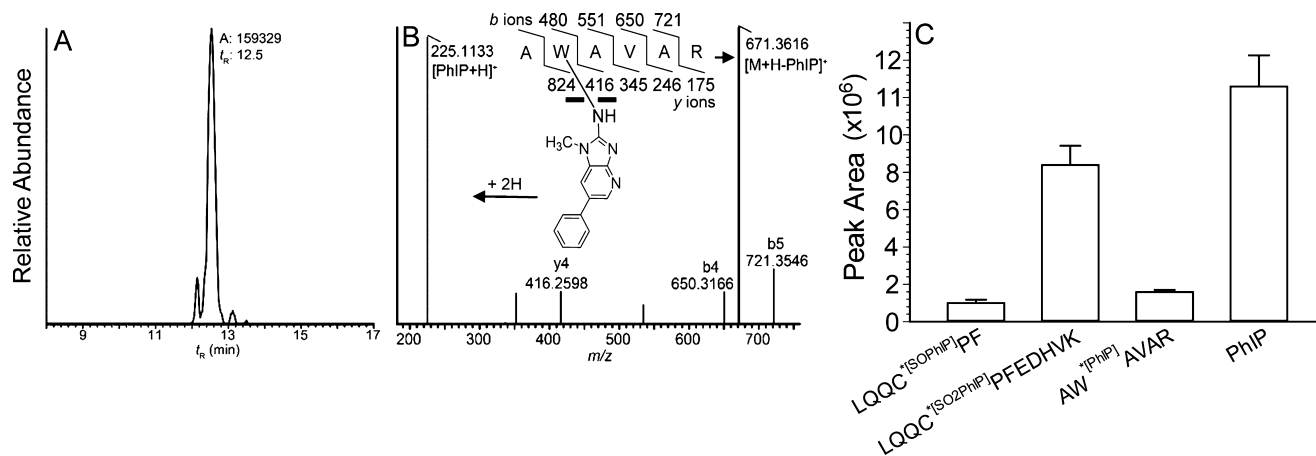


**Figure 5.** (A) Reconstructed mass chromatograms obtained by CID of AW\*[PhIP]AVAR ( $[M+2H]^{2+}$   $m/z$  448.2385 >  $m/z$  225.1135,  $m/z$  671.3624; mass tolerance, 2 ppm) of N-sulfooxy-PhIP-modified albumin digested with trypsin. (B) Product ion spectrum of AW\*[PhIP]AVAR. (C) Relative peak area ion counts of peptide adducts of albumin modified with N-sulfooxy-PhIP: AW\*[PhIP]AVAR recovered from trypsin digest, LQQC\*[SOPhIP]PF ( $[M+2H]^{2+}$  at  $m/z$  487.2 >  $m/z$  225.1,  $m/z$  749.4) and PhIP ( $[M+H]^+$  at  $m/z$  225.1 >  $m/z$  210.0) recovered from trypsin/chymotrypsin digest, and LQQC\*[SO<sub>2</sub>PhIP]PFEDHVK ( $[M+3H]^{3+}$  at  $m/z$  533.2 >  $m/z$  670.2,  $m/z$  679.0) recovered from trypsin/chymotrypsin digestion following m-CPBA oxidation of albumin.

quantitative measurements of the relative amounts of adducts formed cannot be determined and only relative ion abundances

are reported. The AW\*[PhIP]AVAR recovered from a tryptic digest is comparable to the signal of LQQC\*[SO<sub>2</sub>PhIP]PF recovered from the



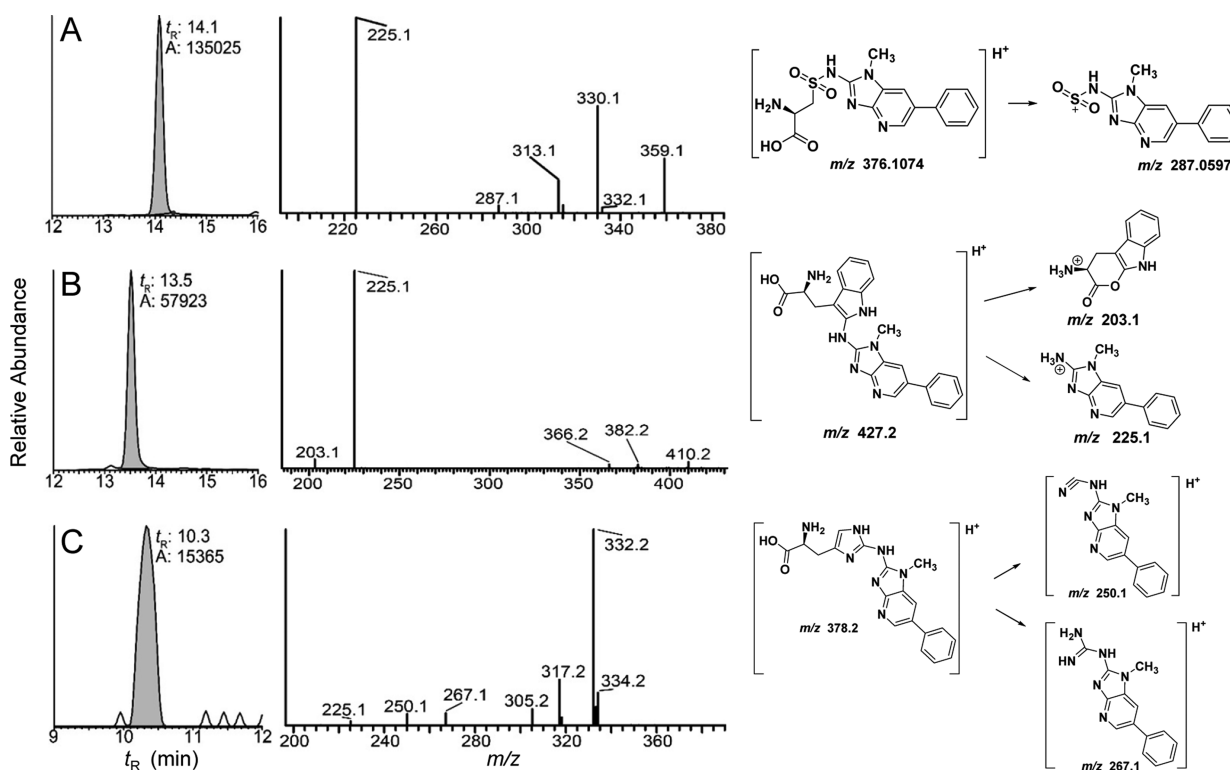


**Figure 6.** Reconstructed mass chromatograms (left) of (A)  $C^{[SO_2PhIP]}$  ( $[M + H]^+$  at  $m/z$  376.1 >  $m/z$  225.1), (B)  $W^{[PhIP]}$  ( $[M + H]^+$  at  $m/z$  421.1 >  $m/z$  225.1), and (C)  $H^{[PhIP]}$  ( $[M + H]^+$  at  $m/z$  378.1 >  $m/z$  225.1,  $m/z$  332.2) from *N*-sulfoxy-PhIP-modified albumin following digestion with Pronase E, leucine aminopeptidase, and prolidase. The product ion mass spectra and proposed diagnostic product ions are depicted (right).

tryptic/chymotryptic digest, but the response is only ~25% of the signal of LQQC\* $^{[SO_2PhIP]}$ PFEDHVK recovered from tryptic/chymotryptic digest (following *m*-CPBA oxidation and stabilization of the Cys<sup>34</sup> S–N-linked PhIP adducts).<sup>39,54,57</sup> The peak area ion count of PhIP, recovered from the tryptic/chymotryptic digest, is 10-fold greater than that of AW\* $^{[PhIP]}$ AVAR (Figure 5C), indicating that a significant proportion of the *N*-sulfoxy-PhIP bound to albumin formed labile Cys<sup>34</sup> S–N linked adducts that underwent hydrolysis during proteolytic digestion.

**Identification of Albumin Adducts of PhIP Formed with Cys, Trp, and His.** PhIP-modified albumin was screened for amino acid adducts in albumin or human plasma reacted with *N*-oxidized metabolites of PhIP:  $^{[2H_5]}$ PhIP, following digestion with Pronase E, leucine aminopeptidase, and prolidase. The  $C^{[SO_2PhIP]}$ ,  $C^{*[SO_2PhIP]}$ PF,  $W^{[PhIP]}$ , and  $H^{[PhIP]}$  from albumin were identified, by the mass tag-triggered data-dependent scan method (Table 1). Subsequently, these adducts were assayed by targeted UPLC–ESI/MS<sup>2</sup>. The mass chromatograms of the adducts formed by reaction of albumin in plasma with *N*-sulfoxy-PhIP are shown in Figure 6. The product ion spectrum of  $C^{[SO_2PhIP]}$  ( $[M + H]^+$  at  $m/z$  376.1) displays a base peak attributed to protonated PhIP ( $m/z$  225.1), an ion at  $m/z$  287.1 due to the charged PhIP-SO<sub>2</sub> moiety ( $[M + H - C_3H_7NO_2]^+$ ); other fragment ions are observed at  $m/z$  313.1 ( $[M + H - NH_3 - H_2CO_2]^+$ ),  $m/z$  330.1 ( $[M + H - H_2CO_2]^+$ ), and  $m/z$  359.1 ( $[M + H - NH_3]^+$ ) (Figure 6A). The  $W^{[PhIP]}$  adduct ( $[M + H]^+$  at  $m/z$  427.1) undergoes CID to produce a minor fragment ion at  $m/z$  203.1 due to the loss of PhIP ( $[M + H - 224]^+$ ); the base peak in the spectrum is protonated PhIP at  $m/z$  225.1. Other fragment ions are observed at  $m/z$  366.2 ( $[M + H - CO_2 - NH_3]^+$ ),  $m/z$  382.2 ( $[M + H - HCO_2]^+$ ),

and  $m/z$  410.2 ( $[M + H - NH_3]^+$ ) (Figure 6B). The mass spectrum is compatible with a structure of an adduct formed between the exocyclic amine group of PhIP and the C-2 atom of the indole group of Trp. The product ion spectrum of the  $H^{[PhIP]}$  adduct ( $[M + H]^+$  at  $m/z$  378.1) is shown in Figure 6C. Fragment ions at occurring at  $m/z$  225.1, 250.1, and 267.1 are consistent with a proposed adduct structure containing a linkage between the exocyclic amine group of PhIP and the C-2 atom of the imidazole ring of His. The product ion spectra of the  $^{[2H_5]}$ PhIP amino acid adducts displayed the same pattern of fragmentation with a shift  $m/z$  5 (data not shown).

The level of  $W^{[PhIP]}$  adduct, based on ion counts, is approximately half the signal of  $C^{[SO_2PhIP]}$ ; however, the ion count of PhIP, formed by hydrolysis of unstable Cys S–N linked adducts, is more than 100 times greater than the ion counts of either  $C^{[SO_2PhIP]}$  or  $W^{[PhIP]}$  recovered from albumin digested with the three-enzyme mixture (Figure 7). The levels of Cys $^{[SO_2PhIP]}$  and Trp $^{[PhIP]}$  are 2 and 3 times greater in *N*-sulfoxy-PhIP-treated than *N*-acetoxy-PhIP- and HONH-PhIP-treated human plasma, respectively (Figure 7A,B). The amount of PhIP recovered from the *N*-sulfoxy-PhIP-modified albumin sample is also ~3 times greater than that from *N*-acetoxy-PhIP- and HONH-PhIP-modified human plasma. The high levels of PhIP recovered from *N*-sulfoxy-PhIP-treated albumin in plasma are indicative of the existence of unstable Cys<sup>34</sup> S–N linked PhIP adducts (Figure 7C). The ion count of  $H^{[PhIP]}$  is 10-fold lower than the ion count of  $C^{[SO_2PhIP]}$  and 5-fold lower than the ion count of  $W^{[PhIP]}$  adducts in *N*-sulfoxy-PhIP-modified albumin (unpublished observations, Y. Wang).

The proficiency of proteolytic digestion of *N*-sulfoxy-PhIP-modified albumin by three enzymes (Pronase E, leucine

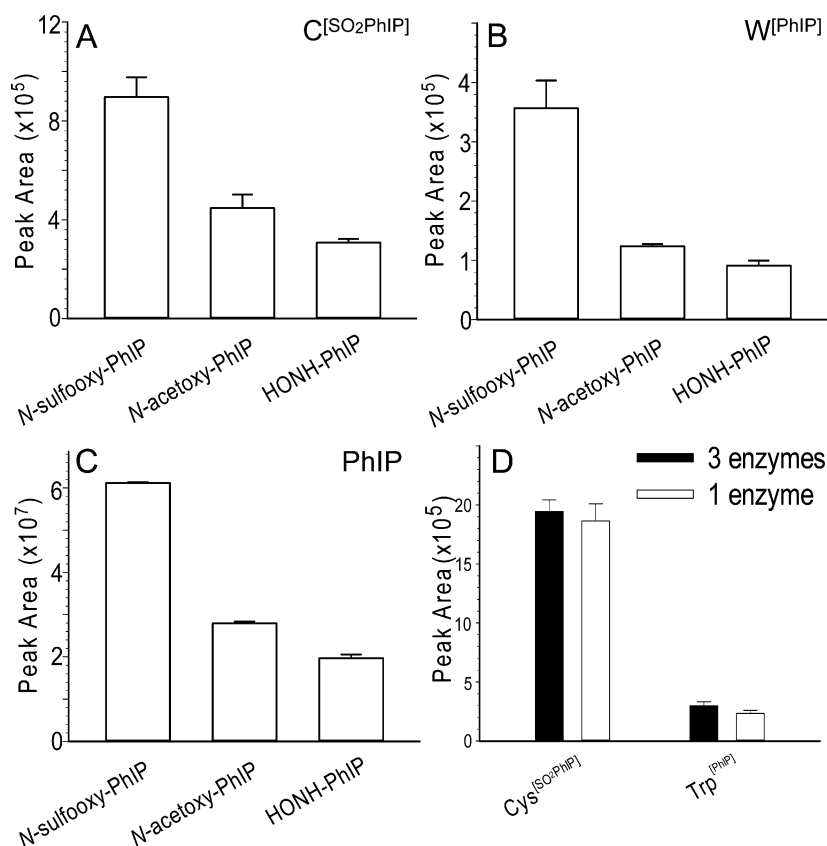


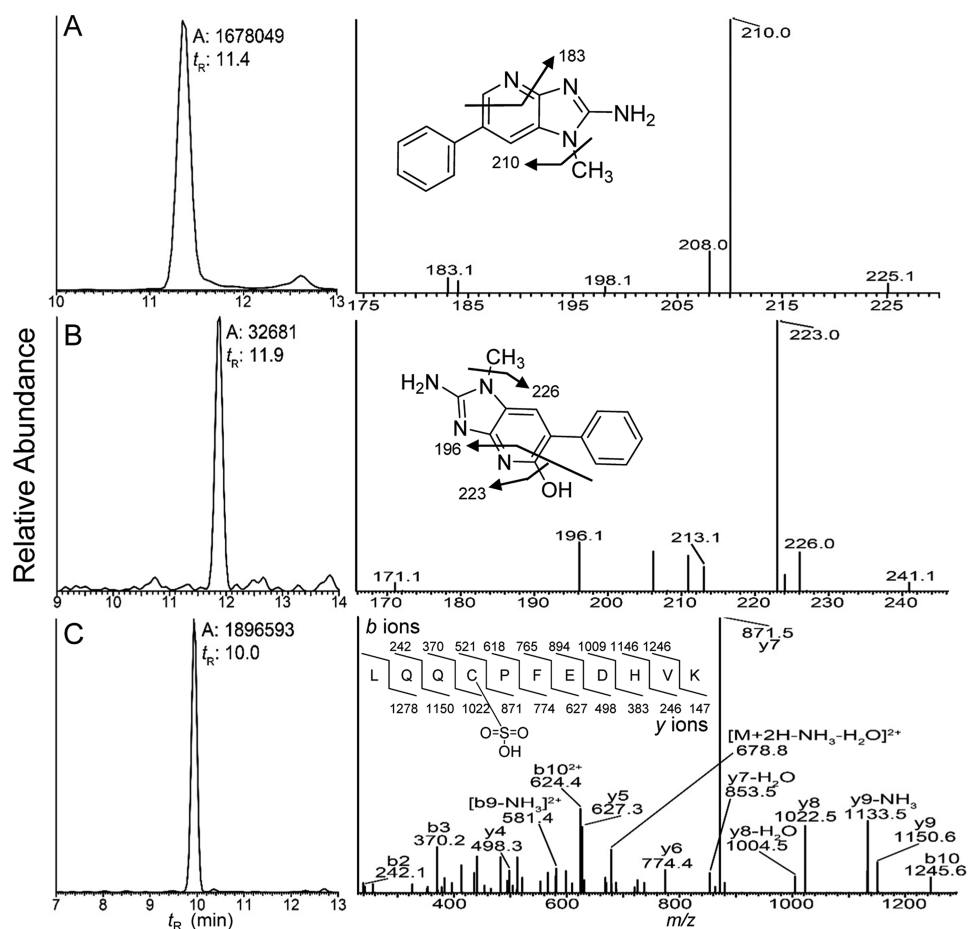
**Figure 7.** (A) Peak area ion count estimates of the UPLC–ESI/MS<sup>2</sup> analysis of (A) C[SO<sub>2</sub>PhIP] ([M + H]<sup>+</sup> at *m/z* 376.1 > *m/z* 225.1), (B) W[PhIP] ([M + H]<sup>+</sup>, *m/z* 421.1 > *m/z* 225.1), and (C) PhIP ([M + H]<sup>+</sup> at *m/z* 225.1 > *m/z* 210.0) recovered from albumin in human plasma modified with *N*-sulfoxy-PhIP following protein digestion with Pronase E, leucine aminopeptidase, and prolidase. (D) Peak area ion count estimates of the UPLC–ESI/MS<sup>2</sup> analysis of C[SO<sub>2</sub>PhIP] ([M + H]<sup>+</sup>, *m/z* 376.1 > *m/z* 225.1) and W[PhIP] ([M + H]<sup>+</sup>, *m/z* 421.1 > *m/z* 225.1) recovered from *N*-sulfoxy-PhIP-modified commercial albumin following digestion with Pronase E, leucine aminopeptidase, and prolidase (black bar), or Pronase E alone (white bar). The albumin digest (200 ng) was injected on column for all samples (mean ± SD; *n* = 3).

aminopeptidase, and prolidase) and one enzyme (Pronase E) on the recovery of C[SO<sub>2</sub>PhIP] and W[PhIP] was examined. In contrast to our previous findings, where C[SO<sub>2</sub>PhIP] was recovered primarily as the tripeptide C[SO<sub>2</sub>PhIP]PF from PhIP-modified commercial albumin digested with this three-enzyme mixture, we saw no significant difference between the amino acid adduct C[SO<sub>2</sub>PhIP] or W[PhIP] levels, when PhIP-modified albumin was digested with three enzymes or Pronase E alone (*p* > 0.05; *t* test) (Figure 7D), and the levels of incompletely digested dipeptide or tripeptide adducts of PhIP were negligible.

**Characterization of Albumin PhIP Adducts and Cys<sup>34</sup>SO<sub>3</sub>H in Human Hepatocytes.** Human hepatocytes were incubated with PhIP (50 μM) or PhIP:[<sup>2</sup>H<sub>5</sub>]PhIP (50 μM, 1:1 ratio) for 24 h and examined for dG-C8-PhIP or albumin adduct formation, respectively. High levels of dG-C8-PhIP adducts were formed: the levels were 10.4 ± 0.3 adducts per 10<sup>6</sup> bases (mean ± SD, three independent measurements), confirming PhIP had undergone extensive bioactivation by P450-mediated N-oxidation in hepatocytes (Figure S-4 of the Supporting Information).<sup>52</sup> However, the mass tag-triggered data-dependent acquisition method failed to detect albumin-PhIP:[<sup>2</sup>H<sub>5</sub>]PhIP adducts. Targeted MS<sup>2</sup> scanning also failed to detect albumin-PhIP peptide adducts at either Cys<sup>34</sup> or Trp<sup>214</sup> following tryptic digestion, tryptic/chymotryptic digestion, or digestion of albumin with the three-enzyme mixture.

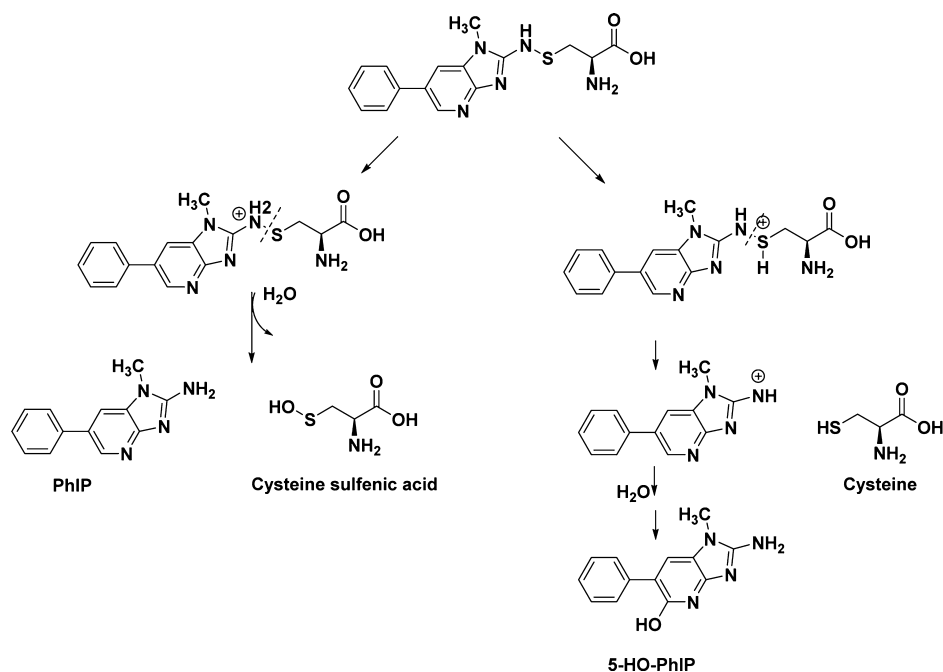
Instead, PhIP and 5-HO-PhIP were detected in the proteolytic digests (Figure 8A,B). Spiking experiments with PhIP in the hepatocyte medium, followed by solvent extraction, proteolytic digestion, and UPLC–ESI/MS<sup>2</sup> targeting for PhIP, showed that all of the spiked PhIP had been removed during the albumin workup (unpublished observations, Y. Wang). These findings suggest the presence of labile Cys<sup>34</sup> S–N linked PhIP adducts, which underwent hydrolysis during proteolytic digestion to form PhIP and 5-HO-PhIP (Scheme 1). The albumin isolated from hepatocytes was oxidized with *m*-CPBA to convert labile Cys<sup>34</sup> S–N linked adducts of PhIP to the stable sulfonamide adducts;<sup>39,54</sup> however, targeted MS<sup>2</sup> scanning failed to detect LQQC\*[SO<sub>2</sub>PhIP]PFEDHVK. The signal of the PhIP sulfonamide adduct is more than 10-fold weaker in response than the signal for PhIP under ESI/MS<sup>2</sup> conditions.<sup>54</sup> We surmise that the level of the sulfonamide adduct is below the limit of detection under our current UPLC–ESI/MS conditions.

HONH-PhIP undergoes oxidation to form nitroso-PhIP, and a redox cycling mechanism with the generation ROS can occur.<sup>58,59</sup> In this study, we discovered that the level of LQQC\*[SO<sub>3</sub>H]PFEDHVK is increased by 6-fold in PhIP-treated hepatocytes compared to the control (*p* < 0.001; *t* test) (unpublished results, Y. Wang). The UPLC/MS chromatogram and product ion spectrum of LQQC\*[SO<sub>3</sub>H]PFEDHVK are shown in Figure 8C. Thus, in addition to the formation of macromolecular adducts, N-oxidized PhIP metabolites induce



**Figure 8.** Reconstructed mass chromatograms (left) of (A) PhIP ( $[M + H]^+$  at  $m/z$  225.1 >  $m/z$  210.0), (B) 5-HO-PhIP ( $[M + H]^+$  at  $m/z$  242.1 >  $m/z$  223.1), and (C) LQQC\* $[\text{SO}_3\text{H}]$ PFEDHVK ( $[M + 2H]^{2+}$  at  $m/z$  696.3 >  $m/z$  871.4,  $m/z$  1022.3) from hepatocytes treated with PhIP, and the corresponding mass spectra (right).

### Scheme 1. Proposed Mechanism of Hydrolysis of Cys<sup>34</sup> PhIP-Sulfenamide To Produce PhIP and 5-HO-PhIP



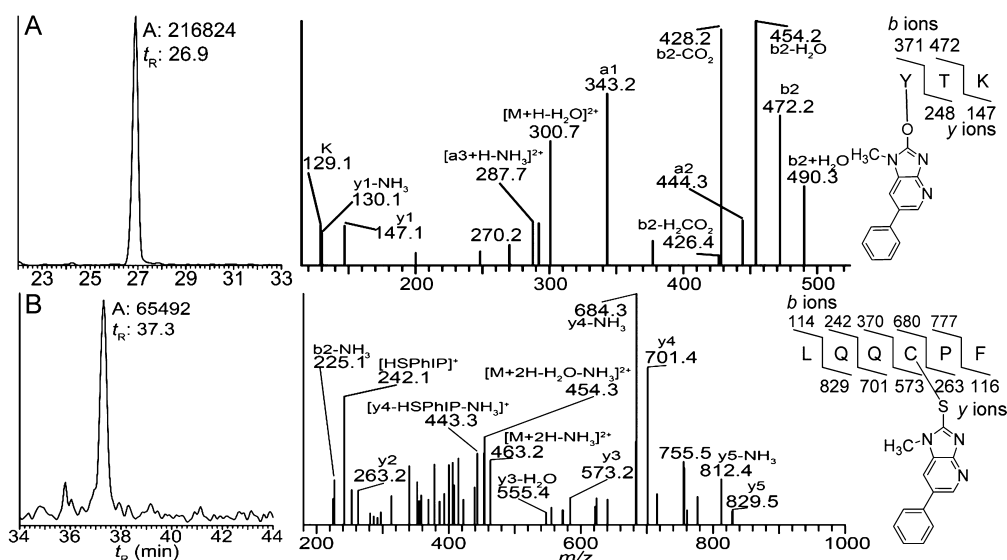


**Figure 9.** Reconstructed mass chromatograms (left) of (A)  $Y^*[\text{desaminoPhIP}]TK$  ( $[M + 2H]^{2+}$  at  $m/z = 309.7 > m/z = 343.2, m/z = 428.3$ ) and (B)  $LQQC^*[\text{desaminoPhIP}]PF$  ( $[M + 2H]^{2+}$  at  $m/z = 471.7 > m/z = 684.3, m/z = 701.3$ ) from human hepatocytes treated with PhIP (50 μM), and the corresponding mass spectra (right).

oxidative stress in human hepatocytes, and Cys<sup>34</sup> of albumin is acting as a scavenger of ROS.

We previously characterized several albumin adduction products formed between commercial human albumin and  $NO_2$ -PhIP.<sup>37</sup> The  $NO_2$  moiety of  $NO_2$ -PhIP undergoes nucleophilic displacement by the HS group of Cys<sup>34</sup> and the HO group of Tyr<sup>411</sup> of albumin to form  $LQQC^*[\text{desaminoPhIP}]PF$  and  $Y^*[\text{desaminoPhIP}]TK$ , respectively, following tryptic/chymotryptic digestion.<sup>37</sup> We screened albumin in human hepatocytes treated with PhIP for  $Y^*[\text{desaminoPhIP}]TK$  and  $LQQC^*[\text{desaminoPhIP}]PF$ , and both adducts were identified (Figure 9).

## DISCUSSION

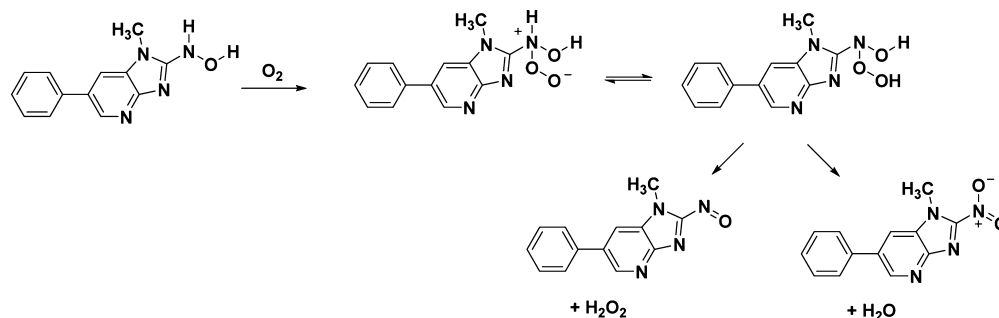
PhIP undergoes extensive bioactivation through P450-mediated N-oxidation to form HONH-PhIP as a major pathway of metabolism in humans.<sup>22–24</sup> In our goal to establish albumin adducts of PhIP as biomarkers for human studies, we have characterized the adduction products of the major N-oxidized metabolites of PhIP, including HONH-PhIP,  $NO$ -PhIP,  $N$ -acetoxy-PhIP, and  $N$ -sulfoxy-PhIP with albumin.<sup>37–39,54</sup> Our findings show that Cys<sup>34</sup> is the principal nucleophile of albumin to react with all of these N-oxidized metabolites of PhIP, to form a putative sulfenamide, and more stable sulfinamide- and sulfonamide-linked adducts.<sup>37–39</sup> Crystallography and NMR studies with human albumin have shown that the Cys<sup>34</sup> resides in a shallow crevice of the protein,<sup>60–62</sup> but it is accessible to solvent. Moreover, the Cys<sup>34</sup> residue of albumin has an unusually low  $pK_a$  value, 6.5, compared to approximately 8.0–8.5 in many other proteins or peptides,<sup>20,63</sup> and it predominantly exists as the thiolate anion at physiological pH, which explains its reactivity toward N-oxidized PhIP metabolites and many other electrophiles.<sup>21</sup>

Trp<sup>214</sup> was identified as a secondary binding site of albumin for N-oxidized metabolites of PhIP, and the hexapeptide adduct  $AW^*[\text{PhIP}]AVAR$  was recovered from a tryptic digest. Trp<sup>214</sup> is not located on the surface of albumin, but it resides in a hydrophobic cavity of subdomain IIA, which is the principal region of ligand binding of human albumin.<sup>61,64</sup> Surprisingly, the

recovery of  $AW^*[\text{PhIP}]AVAR$ , by tryptic digestion, was not increased by denaturation of albumin prior to proteolysis. A previous study in rats dosed with 4-ABP identified Trp<sup>214</sup> of albumin as a major site of adduction of an activated form of the hydroxamic acid of  $N$ -acetyl-4-ABP.<sup>42</sup> The synthetic sulfate esters of  $N$ -hydroxy- $N$ -acetyl-4-ABP,  $N$ -hydroxy- $N$ -acetyl-2-aminofluorene, and  $N$ -hydroxy- $N,N'$ -diacetylbenzidine were also found to bind to Trp<sup>214</sup> of commercial human albumin and recovered as  $AW^*AV$  following Pronase digestion.<sup>26</sup> Most recently, an activated metabolite of Nevirapine, a non-nucleoside reverse transcriptase inhibitor, was reported to bind to Trp<sup>214</sup> of human albumin.<sup>65</sup> Our data show that various N-oxidized metabolites of PhIP react with Trp<sup>214</sup> of albumin. The potential of Trp<sup>214</sup> of albumin to serve as a target site of genotoxants and electrophiles for human biomonitoring has not been explored.

We extended our findings on the reactivity of DNA and albumin with N-oxidized metabolites of PhIP in solution to studies in human hepatocytes. PhIP undergoes bioactivation in hepatocytes, and high levels of dG-C8-PhIP are formed ( $10.4 \pm 0.3$  adducts per  $10^6$  DNA bases); however, levels of Cys<sup>34</sup> or Trp<sup>214</sup> adducts were below the limit of detection. Instead, PhIP and 5-HO-PhIP were recovered from the proteolytic digest of albumin. PhIP and 5-HO-PhIP were also recovered from Pronase digests of rat albumin modified with  $N$ -acetoxy-PhIP.<sup>35</sup> These data suggest that a labile Cys S–N linked sulfenamide adduct of PhIP had formed with albumin and underwent hydrolysis during proteolytic digestion (Scheme 1).<sup>39</sup> The oxidation of PhIP-modified albumin by  $m$ -CPBA converts labile Cys S–N linked adducts to the sulfonamide linkage, which is stable toward proteolytic digestion.<sup>39</sup> We oxidized the albumin isolated from human hepatocytes with  $m$ -CPBA prior to enzyme digestion, and the level of PhIP and 5-HO-PhIP liberated during proteolysis did decrease by severalfold. However,  $LQQC^*[\text{SO}_2\text{PhIP}]PFEDHVK$  was not detected, suggesting that the level of sulfonamide adduct is below the detection limit or the efficacy of oxidation by  $m$ -CPBA was somehow inhibited by components co-extracted with albumin from human hepatocytes.



Scheme 2. A Proposed Reactive N-Hydroperoxy Intermediate of HONH-PhIP That Collapses To Form NO<sub>2</sub>-PhIP<sup>66</sup>

We did, however, detect albumin-PhIP peptide adducts formed with Tyr<sup>411</sup> (Y\*<sup>[desaminoPhIP]</sup>TK) and Cys<sup>34</sup> (LQQC\*<sup>[desaminoPhIP]</sup>PF), where the exocyclic amino moiety of PhIP was displaced by the nucleophilic HO group of Tyr and the HS group of Cys. We previously reported that NO<sub>2</sub>-PhIP undergoes nucleophilic substitution by Tyr<sup>411</sup> and Cys<sup>34</sup> residues of human albumin *in vitro*.<sup>38</sup> The Y\*<sup>[desaminoPhIP]</sup>TK and LQQC\*<sup>[desaminoPhIP]</sup>PF formed in hepatocytes most likely arise from the reaction of NO<sub>2</sub>-PhIP with albumin. Arylhydroxylamines undergo oxidation to form their nitroso and nitro derivatives under aerobic conditions.<sup>66</sup> HONH-PhIP also undergoes oxidation under these conditions to form NO<sub>2</sub>-PhIP (unpublished observations, R. Turesky). A proposed mechanism for NO<sub>2</sub>-PhIP formation is shown in Scheme 2. Consistent with our findings, a desamino glutathione PhIP conjugate was characterized in hepatocytes and bile of rats pretreated with polychlorinated biphenyls.<sup>67</sup>

The response of the ESI/MS signal for the PhIP-DNA adduct, dG-C8-PhIP, is far greater than the signals obtained for albumin-PhIP peptide adducts. However, the amounts of DNA and albumin in hepatocyte culture differ, and the relative reactivity of N-oxidized PhIP with DNA and albumin is difficult to determine, particularly in the absence of internal standards for quantitative measurements of PhIP-albumin adducts. Also, the relative abundances of these macromolecules differ. There is approximately 15 μg of nuclear DNA (45 nmol of DNA bases) per 10<sup>6</sup> hepatocytes, whereas only ~1 μg of albumin (15 pmol albumin) is secreted into the medium per day per 10<sup>6</sup> hepatocytes.<sup>68</sup> In addition, the cell media contain 1 mg/mL exogenously added albumin, and thus, the albumin secreted into the media is diluted by ~1000-fold. Currently, we do not know if PhIP-albumin adduct formation occurs primarily by reaction of N-oxidized PhIP intermediates with newly synthesized albumin within the hepatocyte or with albumin residing in the extracellular media.

In addition to macromolecular adduct formation, N-oxidized PhIP metabolites form reactive oxygen species (ROS) that can oxidize protein and induce toxicity.<sup>58,59</sup> HONH-PhIP can undergo oxidation by P450, transition metals, or oxygen to form NO-PhIP and ROS, and a redox cycling mechanism catalyzed by NADPH-P450 reductase can regenerate HONH-PhIP.<sup>58</sup> There was a 6-fold increase in the levels of the sulfonic acid at Cys<sup>34</sup> of albumin, and LQQC\*<sup>[SO<sub>3</sub>H]</sup>PFEDHVK was detected in hepatocytes treated with PhIP. Thus, Cys<sup>34</sup> of albumin serves as an antioxidant and scavenger of free radicals induced by metabolites of PhIP in human hepatocytes.

In a summary, amino acid and peptide adducts of Cys<sup>34</sup>, Trp<sup>214</sup>, LQQC\*<sup>[SOPHIP]</sup>PF, LQQC\*<sup>[SOPHIP]</sup>PFEDHVK, LQQC\*<sup>[SO<sub>2</sub>PhIP]</sup>PFEDHVK, AW\*<sup>[PhIP]</sup>AVAR, Y<sup>411</sup>\*<sup>[desaminoPhIP]</sup>TK, and LQQC\*<sup>[desaminoPhIP]</sup>PF were identified

in human albumin reacted with N-oxidized metabolites of PhIP. We plan to determine whether these albumin peptide adducts may be candidate protein biomarkers of PhIP in humans.

## ■ ASSOCIATED CONTENT

### ■ Supporting Information

UV spectra of PhIP, HONH-PhIP, and N-acetoxy-PhIP; product ion spectra of N-acetoxy-PhIP and fragmentation mechanism; and mass chromatogram and product ion spectra of dG-C8-PhIP obtained by the reaction of dG with N-sulfooxy-PhIP and human hepatocytes treated with PhIP. This material is available free of charge via the Internet at <http://pubs.acs.org>.

## ■ AUTHOR INFORMATION

### Corresponding Author

\*Masonic Cancer Center and Department of Medicinal Chemistry, Cancer and Cardiology Research Building, University of Minnesota, 2231 6th St., Minneapolis, MN 55455. Telephone: +1 612-626-0141. Fax: +1 612-624-3869.

### Funding

This research was supported by Grant 2R01 CA122320 (R.J.T.) and in part by National Cancer Institute Cancer Center Support Grant CA-77598 (R.J.T.) and the PNREST Anses, Cancer TMOI AVIESAN, 2013/1/166 (S.L.).

### Notes

The authors declare no competing financial interest.

## ■ ACKNOWLEDGMENTS

We thank the Dr. David Tabb Laboratory at the Department of Biomedical Informatics, and the Department of Biochemistry and Mass Spectrometry Research Center, Vanderbilt University (Nashville, TN), for the introduction to and use of the MyriMatch software program. We acknowledge the Centre de Ressources Biologiques (CRB)-Santé of Rennes for managing the patient samples.

## ■ ABBREVIATIONS

PhIP, 2-amino-1-methyl-6-phenylimidazo[4,5-b]pyridine; 5-HO-PhIP, 2-amino-1-methyl-6-(5-hydroxy)phenylimidazo[4,5-b]pyridine; N-acetoxy-PhIP, N-(acetyloxy)-2-amino-1-methyl-6-phenylimidazo[4,5-b]pyridine; HONH-PhIP, 2-hydroxyamino-1-methyl-6-phenylimidazo[4,5-b]pyridine; NO-PhIP, 2-nitroso-1-methyl-6-phenylimidazo[4,5-b]pyridine; NO<sub>2</sub>-PhIP, 2-nitro-1-methyl-6-phenylimidazo[4,5-b]pyridine; N-sulfooxy-PhIP, N-sulfooxy-2-amino-1-methyl-6-phenylimidazo[4,5-b]pyridine; Hb, hemoglobin; HAA, heterocyclic aromatic amine; HCD, higher-energy collisional dissociation; m-CPBA, m-chloroperoxybenzoic acid; UPLC-ESI/MS/MS, ultraperformance liquid

chromatography–tandem mass spectrometry;  $\beta$ ME,  $\beta$ -mercaptoethanol; SPE, solid-phase extraction; dG, deoxyguanosine; dR, deoxyribose

## REFERENCES

- (1) Sugimura, T., Wakabayashi, K., Nakagama, H., and Nagao, M. (2004) Heterocyclic amines: Mutagens/carcinogens produced during cooking of meat and fish. *Cancer Sci.* 95, 290–299.
- (2) Felton, J. S., Jagerstad, M., Knize, M. G., Skog, K., and Wakabayashi, K. (2000) Contents in foods, beverages and tobacco. In *Food Borne Carcinogens Heterocyclic Amines* (Nagao, M., and Sugimura, T., Eds.) pp 31–71, John Wiley & Sons Ltd., Chichester, England.
- (3) Knize, M. G., Dolbeare, F. A., Carroll, K. L., Moore, D. H., and Felton, J. S. (1994) Effect of cooking time and temperature on the heterocyclic amine content of fried beef patties. *Food Chem. Toxicol.* 32, 595–603.
- (4) Sinha, R., Rothman, N., Brown, E. D., Salmon, C. P., Knize, M. G., Swanson, C. S., Rossi, S. C., Mark, S. D., Levander, O. A., and Felton, J. S. (1995) High concentrations of the carcinogen 2-amino-1-methyl-6-phenylimidazo[4,5-*b*]pyridine (PhIP) occur in chicken but are dependent on the cooking method. *Cancer Res.* 55, 4516–4519.
- (5) Zhao, K., Murray, S., Davies, D. S., Boobis, A. R., and Gooderham, N. J. (1994) Metabolism of the food derived mutagen and carcinogen 2-amino-1-methyl-6-phenylimidazo[4,5-*b*]pyridine (PhIP) by human liver microsomes. *Carcinogenesis* 15, 1285–1288.
- (6) Turesky, R. J., Constable, A., Richoz, J., Varga, N., Markovic, J., Martin, M. V., and Guengerich, F. P. (1998) Activation of heterocyclic aromatic amines by rat and human liver microsomes and by purified rat and human cytochrome P450 1A2. *Chem. Res. Toxicol.* 11, 925–936.
- (7) Kato, R. (1986) Metabolic activation of mutagenic heterocyclic aromatic amines from protein pyrolysates. *CRC Crit. Rev. Toxicol.* 16, 307–348.
- (8) Nguyen, T. M., and Novak, M. (2007) Synthesis and decomposition of an ester derivative of the procarcinogen and promutagen, PhIP, 2-amino-1-methyl-6-phenyl-1H-imidazo[4,5-*b*]pyridine: Unusual nitrenium ion chemistry. *J. Org. Chem.* 72, 4698–4706.
- (9) Turesky, R. J., and Le Marchand, L. (2011) Metabolism and biomarkers of heterocyclic aromatic amines in molecular epidemiology studies: Lessons learned from aromatic amines. *Chem. Res. Toxicol.* 24, 1169–1214.
- (10) Lin, D., Kaderlik, K. R., Turesky, R. J., Miller, D. W., Lay, J. O., Jr., and Kadlubar, F. F. (1992) Identification of N-(deoxyguanosin-8-yl)-2-amino-1-methyl-6-phenylimidazo[4,5-*b*]pyridine as the major adduct formed by the food-borne carcinogen, 2-amino-1-methyl-6-phenylimidazo[4,5-*b*]pyridine, with DNA. *Chem. Res. Toxicol.* 5, 691–697.
- (11) Goodenough, A. K., Schut, H. A., and Turesky, R. J. (2007) Novel LC-ESI/MS/MS<sup>n</sup> method for the characterization and quantification of 2'-deoxyguanosine adducts of the dietary carcinogen 2-amino-1-methyl-6-phenylimidazo[4,5-*b*]pyridine by 2-D linear quadrupole ion trap mass spectrometry. *Chem. Res. Toxicol.* 20, 263–276.
- (12) Gu, D., Turesky, R. J., Tao, Y., Langouet, S. A., Nauwelaers, G. C., Yuan, J. M., Yee, D., and Yu, M. C. (2012) DNA adducts of 2-amino-1-methyl-6-phenylimidazo[4,5-*b*]pyridine and 4-aminobiphenyl are infrequently detected in human mammary tissue by liquid chromatography/tandem mass spectrometry. *Carcinogenesis* 33, 124–130.
- (13) Bessette, E. E., Spivack, S. D., Goodenough, A. K., Wang, T., Pinto, S., Kadlubar, F. F., and Turesky, R. J. (2010) Identification of carcinogen DNA adducts in human saliva by linear quadrupole ion trap/multistage tandem mass spectrometry. *Chem. Res. Toxicol.* 23, 1234–1244.
- (14) Tretyakova, N., Goggin, M., Sangaraju, D., and Janis, G. (2012) Quantitation of DNA adducts by stable isotope dilution mass spectrometry. *Chem. Res. Toxicol.* 25, 2007–2035.
- (15) Miller, J. A. (1970) Carcinogenesis by chemicals: An overview—G. H. A. Clowes memorial lecture. *Cancer Res.* 30, 559–576.
- (16) Rubino, F. M., Pitton, M., Di, F. D., and Colombi, A. (2009) Toward an “omic” physiopathology of reactive chemicals: Thirty years of mass spectrometric study of the protein adducts with endogenous and xenobiotic compounds. *Mass Spectrom. Rev.* 28, 725–784.
- (17) Tornqvist, M., Fred, C., Haglund, J., Helleberg, H., Paulsson, B., and Rydberg, P. (2002) Protein adducts: Quantitative and qualitative aspects of their formation, analysis and applications. *J. Chromatogr. B: Anal. Technol. Biomed. Life Sci.* 778, 279–308.
- (18) Skipper, P. L., and Tannenbaum, S. R. (1990) Protein adducts in the molecular dosimetry of chemical carcinogens. *Carcinogenesis* 11, 507–518.
- (19) Liebler, D. C. (2002) Proteomic approaches to characterize protein modifications: New tools to study the effects of environmental exposures. *Environ. Health Perspect.* 110 (Suppl. 1), 3–9.
- (20) Aldini, G., Regazzoni, L., Orioli, M., Rimoldi, I., Facino, R. M., and Carini, M. (2008) A tandem MS precursor-ion scan approach to identify variable covalent modification of albumin Cys<sup>34</sup>: A new tool for studying vascular carbonylation. *J. Mass Spectrom.* 43, 1470–1481.
- (21) Rappaport, S. M., Li, H., Grigoryan, H., Funk, W. E., and Williams, E. R. (2012) Adductomics: Characterizing exposures to reactive electrophiles. *Toxicol. Lett.* 213, 83–90.
- (22) Malfatti, M. A., Dingley, K. H., Nowell-Kadlubar, S., Ubick, E. A., Mulakken, N., Nelson, D., Lang, N. P., Felton, J. S., and Turteltaub, K. W. (2006) The urinary metabolite profile of the dietary carcinogen 2-amino-1-methyl-6-phenylimidazo[4,5-*b*]pyridine is predictive of colon DNA adducts after a low-dose exposure in humans. *Cancer Res.* 66, 10541–10547.
- (23) Walters, D. G., Young, P. J., Agus, C., Knize, M. G., Boobis, A. R., Gooderham, N. J., and Lake, B. G. (2004) Cruciferous vegetable consumption alters the metabolism of the dietary carcinogen 2-amino-1-methyl-6-phenylimidazo[4,5-*b*]pyridine (PhIP) in humans. *Carcinogenesis* 25, 1659–1669.
- (24) Gu, D., McNaughton, L., LeMaster, D., Lake, B. G., Gooderham, N. J., Kadlubar, F. F., and Turesky, R. J. (2010) A comprehensive approach to the profiling of the cooked meat carcinogens 2-amino-3,8-dimethylimidazo[4,5-*f*]quinoxaline, 2-amino-1-methyl-6-phenylimidazo[4,5-*b*]pyridine, and their metabolites in human urine. *Chem. Res. Toxicol.* 23, 788–801.
- (25) Kiese, M. (1966) The biochemical production of ferrihemoglobin-forming derivatives from aromatic amines, and mechanisms of ferrihemoglobin formation. *Pharmacol. Rev.* 18, 1091–1161.
- (26) Tannenbaum, S. R., Skipper, P. L., Wishnok, J. S., Stillwell, W. G., Day, B. W., and Taghizadeh, K. (1993) Characterization of various classes of protein adducts. *Environ. Health Perspect.* 99, 51–55.
- (27) Yu, M. C., Skipper, P. L., Tannenbaum, S. R., Chan, K. K., and Ross, R. K. (2002) Arylamine exposures and bladder cancer risk. *Mutat. Res.* 506–507, 21–28.
- (28) Ringe, D., Turesky, R. J., Skipper, P. L., and Tannenbaum, S. R. (1988) Structure of the single stable hemoglobin adduct formed by 4-aminobiphenyl *in vivo*. *Chem. Res. Toxicol.* 1, 22–24.
- (29) Dingley, K. H., Curtis, K. D., Nowell, S., Felton, J. S., Lang, N. P., and Turteltaub, K. W. (1999) DNA and protein adduct formation in the colon and blood of humans after exposure to a dietary-relevant dose of 2-amino-1-methyl-6-phenylimidazo[4,5-*b*]pyridine. *Cancer Epidemiol. Biomarkers Prev.* 8, 507–512.
- (30) Garner, R. C., Lightfoot, T. J., Cupid, B. C., Russell, D., Coxhead, J. M., Kutschera, W., Priller, A., Rom, W., Steier, P., Alexander, D. J., Leveson, S. H., Dingley, K. H., Mauthe, R. J., and Turteltaub, K. W. (1999) Comparative biotransformation studies of MeIQx and PhIP in animal models and humans. *Cancer Lett.* 143, 161–165.
- (31) Peters, T., Jr. (1985) Serum albumin. *Adv. Protein Chem.* 37, 161–245.
- (32) Colombo, G., Clerici, M., Giustarini, D., Rossi, R., Milzani, A., and Dalle-Donne, I. (2012) Redox albuminomics: Oxidized albumin in human diseases. *Antioxid. Redox Signaling* 17, 1515–1527.
- (33) Turesky, R. J., Skipper, P. L., and Tannenbaum, S. R. (1987) Binding of 2-amino-3-methylimidazo[4,5-*f*]quinoline to hemoglobin and albumin *in vivo* in the rat. Identification of an adduct suitable for dosimetry. *Carcinogenesis* 8, 1537–1542.

- (34) Lynch, A. M., Murray, S., Boobis, A. R., Davies, D. S., and Gooderham, N. J. (1991) The measurement of MeIQx adducts with mouse haemoglobin *in vitro* and *in vivo*: Implications for human dosimetry. *Carcinogenesis* 12, 1067–1072.
- (35) Reistad, R., Frandsen, H., Grivas, S., and Alexander, J. (1994) *In vitro* formation and degradation of 2-amino-1-methyl-6-phenylimidazo[4,5-b]pyridine (PhIP) protein adducts. *Carcinogenesis* 15, 2547–2552.
- (36) Chepanoske, C. L., Brown, K., Turteltaub, K. W., and Dingley, K. H. (2004) Characterization of a peptide adduct formed by N-acetoxy-2-amino-1-methyl-6-phenylimidazo[4,5-b]pyridine (PhIP), a reactive intermediate of the food carcinogen PhIP. *Food Chem. Toxicol.* 42, 1367–1372.
- (37) Peng, L., and Turesky, R. J. (2011) Mass spectrometric characterization of 2-amino-1-methyl-6-phenylimidazo[4,5-b]pyridine N-oxidized metabolites bound at Cys<sup>34</sup> of human serum albumin. *Chem. Res. Toxicol.* 24, 2004–2017.
- (38) Peng, L., Dasari, S., Tabb, D. L., and Turesky, R. J. (2012) Mapping serum albumin adducts of the food-borne carcinogen 2-amino-1-methyl-6-phenylimidazo[4,5-b]pyridine by data-dependent tandem mass spectrometry. *Chem. Res. Toxicol.* 25, 2179–2193.
- (39) Peng, L., and Turesky, R. J. (2013) Capturing labile sulfenamide and sulfenamide serum albumin adducts of carcinogenic arylamines by chemical oxidation. *Anal. Chem.* 85, 1065–1072.
- (40) Frandsen, H., Grivas, S., Andersson, R., Dragsted, L., and Larsen, J. C. (1992) Reaction of the N2-acetoxy derivative of 2-amino-1-methyl-6-phenylimidazo[4,5-b]pyridine (PhIP) with 2'-deoxyguanosine and DNA. Synthesis and identification of N<sup>2</sup>-(2'-deoxyguanosin-8-yl)-PhIP. *Carcinogenesis* 13, 629–635.
- (41) Skipper, P. L. (1996) Influence of tertiary structure on nucleophilic substitution reactions of proteins. *Chem. Res. Toxicol.* 9, 918–923.
- (42) Skipper, P. L., Obiedzinski, M. W., Tannenbaum, S. R., Miller, D. W., Mitchum, R. K., and Kadlubar, F. F. (1985) Identification of the major serum albumin adduct formed by 4-aminobiphenyl *in vivo* in rats. *Cancer Res.* 45, 5122–5127.
- (43) Wu, R. W., Tucker, J. D., Sorensen, K. J., Thompson, L. H., and Felton, J. S. (1997) Differential effect of acetyltransferase expression on the genotoxicity of heterocyclic amines in CHO cells. *Mutat. Res.* 390, 93–103.
- (44) Wu, R. W., Panteleakos, F. N., Kadkhodayan, S., Bolton-Grob, R., McManus, M. E., and Felton, J. S. (2000) Genetically modified Chinese hamster ovary cells for investigating sulfotransferase-mediated cytotoxicity and mutation by 2-amino-1-methyl-6-phenylimidazo[4,5-b]pyridine. *Environ. Mol. Mutagen.* 35, 57–65.
- (45) Metry, K. J., Zhao, S., Neale, J. R., Doll, M. A., States, J. C., McGregor, W. G., Pierce, W. M., Jr., and Hein, D. W. (2007) 2-Amino-1-methyl-6-phenylimidazo[4,5-b]pyridine-induced DNA adducts and genotoxicity in Chinese hamster ovary (CHO) cells expressing human CYP1A2 and rapid or slow acetylator N-acetyltransferase 2. *Mol. Carcinog.* 46, 553–563.
- (46) Nowell, S., Ambrosone, C. B., Ozawa, S., MacLeod, S. L., Mrackova, G., Williams, S., Plaxco, J., Kadlubar, F. F., and Lang, N. P. (2000) Relationship of phenol sulfotransferase activity (SULT1A1) genotype to sulfotransferase phenotype in platelet cytosol. *Pharmacogenetics* 10, 789–797.
- (47) Dobbernack, G., Meinel, W., Schade, N., Florian, S., Wend, K., Voigt, I., Himmelbauer, H., Gross, M., Liehr, T., and Glatt, H. (2011) Altered tissue distribution of 2-amino-1-methyl-6-phenylimidazo[4,5-b]pyridine-DNA adducts in mice transgenic for human sulfotransferases 1A1 and 1A2. *Carcinogenesis* 32, 1734–1740.
- (48) Turesky, R. J., Lang, N. P., Butler, M. A., Teitel, C. H., and Kadlubar, F. F. (1991) Metabolic activation of carcinogenic heterocyclic aromatic amines by human liver and colon. *Carcinogenesis* 12, 1839–1845.
- (49) Langouët, S., Paehler, A., Welti, D. H., Kerriguy, N., Guillouzo, A., and Turesky, R. J. (2002) Differential metabolism of 2-amino-1-methyl-6-phenylimidazo[4,5-b]pyridine in rat and human hepatocytes. *Carcinogenesis* 23, 115–122.
- (50) Attaluri, S., Iden, C. R., Bonala, R. R., and Johnson, F. (2014) Total synthesis of the aristolochic acids, their major metabolites, and related compounds. *Chem. Res. Toxicol.* 27, 1236–1242.
- (51) Beland, F. A., Miller, D. W., and Mitchum, R. K. (1983) Synthesis of the ultimate hepatocarcinogen 2-acetylaminofluorene N-sulphate. *J. Chem. Soc., Chem. Commun.*, 30–31.
- (52) Nauwelaers, G., Bessette, E. E., Gu, D., Tang, Y., Rageul, J., Fessard, V., Yuan, J. M., Yu, M. C., Langouët, S., and Turesky, R. J. (2011) DNA adduct formation of 4-aminobiphenyl and heterocyclic aromatic amines in human hepatocytes. *Chem. Res. Toxicol.* 24, 913–925.
- (53) Tabb, D. L., Fernando, C. G., and Chambers, M. C. (2007) MyriMatch: Highly accurate tandem mass spectral peptide identification by multivariate hypergeometric analysis. *J. Proteome Res.* 6, 654–661.
- (54) Peng, L., and Turesky, R. J. (2014) Optimizing proteolytic digestion conditions for the analysis of serum albumin adducts of 2-amino-1-methyl-6-phenylimidazo[4,5-b]pyridine, a potential human carcinogen formed in cooked meat. *J. Proteomics* 30, 267–278.
- (55) Fede, J. M., Thakur, A. P., Gooderham, N. J., and Turesky, R. J. (2009) Biomonitoring of 2-amino-1-methyl-6-phenylimidazo[4,5-b]pyridine (PhIP) and its carcinogenic metabolites in urine. *Chem. Res. Toxicol.* 22, 1096–1105.
- (56) Chen, C., Ma, X., Malfatti, M. A., Krausz, K. W., Kimura, S., Felton, J. S., Idle, J. R., and Gonzalez, F. J. (2007) A comprehensive investigation of 2-amino-1-methyl-6-phenylimidazo[4,5-b]pyridine (PhIP) metabolism in the mouse using a multivariate data analysis approach. *Chem. Res. Toxicol.* 20, 531–542.
- (57) Gan, L. S., Skipper, P. L., Peng, X. C., Groopman, J. D., Chen, J. S., Wogan, G. N., and Tannenbaum, S. R. (1988) Serum albumin adducts in the molecular epidemiology of aflatoxin carcinogenesis: Correlation with aflatoxin B1 intake and urinary excretion of aflatoxin M1. *Carcinogenesis* 9, 1323–1325.
- (58) Kim, D., Kadlubar, F. F., Teitel, C. H., and Guengerich, F. P. (2004) Formation and reduction of aryl and heterocyclic nitroso compounds and significance in the flux of hydroxylamines. *Chem. Res. Toxicol.* 17, 529–536.
- (59) Murata, M., and Kawanishi, S. (2011) Mechanisms of oxidative DNA damage induced by carcinogenic arylamines. *Front. Biosci., Landmark Ed.* 16, 1132–1143.
- (60) Thomas, A. T., Stewart, B. J., Ognibene, T. J., Turteltaub, K. W., and Bench, G. (2013) Directly coupled high-performance liquid chromatography-accelerator mass spectrometry measurement of chemically modified protein and peptides. *Anal. Chem.* 85, 3644–3650.
- (61) Carter, D. C., and Ho, J. X. (1994) Structure of serum albumin. *Adv. Protein Chem.* 45, 153–203.
- (62) Christodoulou, J., and Sadler, P. J. (1995) <sup>1</sup>H NMR of albumin in human blood plasma: Drug binding and redox reactions at Cys34. *FEBS Lett.* 376, 1–5.
- (63) Stewart, A. J., Blindauer, C. A., Berezenko, S., Sleep, D., Tooth, D., and Sadler, P. J. (2005) Role of Tyr84 in controlling the reactivity of Cys34 of human albumin. *FEBS J.* 272, 353–362.
- (64) He, X. M., and Carter, D. C. (1992) Atomic structure and chemistry of human serum albumin. *Nature* 358, 209–215.
- (65) Antunes, A. M., Godinho, A. L., Martins, I. L., Oliveira, M. C., Gomes, R. A., Coelho, A. V., Beland, F. A., and Marques, M. M. (2010) Protein adducts as prospective biomarkers of nevirapine toxicity. *Chem. Res. Toxicol.* 23, 1714–1725.
- (66) Becker, A. R., and Sternson, L. A. (1981) Oxidation of phenylhydroxylamine in aqueous solution: A model for study of the carcinogenic effect of primary aromatic amines. *Proc. Natl. Acad. Sci. U.S.A.* 78, 2003–2007.
- (67) Alexander, J., Wallin, H., Rossland, O. J., Solberg, K. E., Holme, J. A., Becher, G., Andersson, R., and Grivas, S. (1991) Formation of a glutathione conjugate and a semistable transportable glucuronide conjugate of N2-oxidized species of 2-amino-1-methyl-6-phenylimidazo[4,5-b]pyridine (PhIP) in rat liver. *Carcinogenesis* 12, 2239–2245.
- (68) Kostadinova, R., Boess, F., Applegate, D., Suter, L., Weiser, T., Singer, T., Naughton, B., and Roth, A. (2013) A long-term three

dimensional liver co-culture system for improved prediction of clinically relevant drug-induced hepatotoxicity. *Toxicol. Appl. Pharmacol.* 268, 1–16.

(69) Pace, C. N., Vajdos, F., Fee, L., Grimsley, G., and Gray, T. (1995) How to measure and predict the molar absorption coefficient of a protein. *Protein Sci.* 4, 2411–2423.